UNIVERSITÉ DU QUÉBEC À MONTRÉAL

CARACTÉRISTIQUES DES VENTS HORAIRES ET DES RAFALES DE VENTS TELLES QUE SIMULÉES PAR UN MODÈLE RÉGIONAL DU CLIMAT À TRÈS HAUTE RÉSOLUTION

MÉMOIRE

PRÉSENTÉ

COMME EXIGENCE PARTIELLE EN

SCIENCES DE L'ENVIRONNEMENT

PAR

AMÉLIE MICHAUD

JUIN 2026

REMERCIEMENTS

À Philippe Gachon, d'abord pour m'avoir donné la chance de travailler avec lui ; également pour son soutien scientifique et financier. Enfin, pour m'avoir donné l'occasion d'assister à d'excellents congrès, dont celui de CMOS.

À Martin Leduc pour son expertise et l'aide tout le long de mon cheminement. Les conseils et connaissances que vous m'avez transmis furent enrichissants.

À mes collègues du bureau : Milena pour toute l'aide, les discussions intéressantes, même si tu ne comprends pas toujours mon français québécois ; Maxine pour les conseils et le plaisir que nous avons eu ; Tim et Tanguy qui sont toujours là pour m'aider et pour un futur divan… j'espère.

À Sandra pour tous les biscuits, les encouragements ; Clémence, Ana et François pour l'aide avec tous mes problèmes en programmation sans qui je n'aurais pas pu accomplir mon étude.

DÉDICACE

À Laurie,

Yves

et Marie-Andrée

TABLE DES MATIÈRES

LISTE DES FIGURES

LISTE DES TABLEAUX

LISTE DES ABRÉVIATIONS, DES SIGLES ET DES ACRONYMES

ARRIMÉ : Aléas, Risques et Résilience des Infrastructures minières et électriques

ECCC : *Environnement and climate change Canada*

ERA5 : La cinquième génération de réanalyse globale du climat du centre européen pour les prévisions météorologiques à moyen terme

GIEC : Groupe d'experts intergouvernemental sur l'évolution du climat

MAR : Modèle atmosphérique régional

MCS et SCM : Mesoscale convective systems (système convectif de mésoéchelle)

MRCC6 et CRCM6 : Modèle régional canadien du Climat version 6

MRCC6-1S et CRCM6 : Modèle régional canadien du Climat version 6 à 1km de résolution

MRCC6-1L et CRCM6: Modèle régional canadien du Climat version 6 à 1km de résolution appliqué sur le domaine de 2.5km

MRCC6-2.5 et CRCM6 : Modèle régional canadien du Climat version 6 à 2.5km de résolution

MRCC6-12 et CRCM6 : Modèle régional canadien du Climat version 6 à 12km de résolution

PBL: Planetary boundary layer

PDF: probability density function

SD: standard deviation

SS: Skill score

WGE: Wind gust estimation (estimation des rafales de vent)

WGN: Wind gust estimate minimum

WGX: Wind gust estimate maximum

LISTE DES SYMBOLES ET DES UNITÉS

U: Composante zonale (ouest-est) du vent horizontal

V : Composante méridienne (sud-nord) du vent horizontal

m/s: mètre par seconde

km: kilomètre

hPa: Hectopascal

RÉSUMÉ

Les rafales de vent sont la cause principale de dommages et de bris au réseau de distribution d'Hydro-Québec lors des tempêtes intenses. Lors de ces tempêtes, les changements soudains de direction ou de vitesse des vents endommagent les lignes de distribution d'électricité et provoquent des bris de branches ou des chutes d'arbres. Ce sont ces événements qui sont responsables de la majorité des pertes matérielles et des pannes d'électricité sur le territoire québécois. Cette étude a pour objectif d'évaluer la valeur ajoutée de l'utilisation de la très haute résolution de la sixième version du Modèle régional canadien du climat (MRCC6), en mode *convection-permitting*, développé au centre ESCER de l'UQAM dans la simulation des vents intenses et des rafales de vent. Les rafales sont définies comme des épisodes de vitesse de vents extrêmes d'une durée d'environ 3 s, et dont la vitesse surpasse la vitesse les vents moyens d'au moins 5 m/s. Différentes configurations du MRCC6 sont utilisées pour produire les simulations à 12, 2,5 et 1 km de résolution, toutes pilotées à partir de la réanalyse ERA5, dans lesquelles le module de rafales de vent est activé, utilisant la méthode de Brasseur (2001). Ce module permet de diagnostiquer les rafales à l'aide de l'énergie cinétique turbulente, de la stabilité statique ainsi que des caractéristiques de la couche limite. L'analyse de ces simulations se réalise à partir de deux études de cas, soit deux tempêtes, la première synoptique, survenue en décembre 2022, et l'autre de mésoéchelle, en mai 2022, en utilisant les stations d'observation sur le territoire pour comparer les résultats des simulations.

Dans le cas de la tempête synoptique de décembre 2022, le modèle à très haute résolution (2,5 et 1 km) offre de meilleures performances pour estimer les rafales, ainsi que les vents horaires que la simulation à 12 km de résolution ou que la réanalyse ERA5. De plus, le modèle tend à être plus précis sur la mer que sur la terre, ainsi que dans les situations où les vents continus sont plus forts. Dans le cas du derecho de mai 2022, les simulations à très haute résolution présentent une valeur ajoutée moins importante ou systématique que les produits à plus basse résolution, même si la simulation à 1 km de résolution est plus performante en ce qui concerne les vitesses de vent et de rafales.

Mots clés : Rafale de vent, tempête synoptique, derecho, système convectif de mésoéchelle, modélisation du climat à très haute résolution.

ABSTRACT

Wind gusts are one of the primary causes of damage and failures in Hydro-Québec's electricity distribution network during extreme storms, due to the sudden changes in wind speed and direction they generate. These changes cause damage to trees, branches as well as power lines. These events account for most material losses and power outages across Québec. This study aims to assess the added value of very high horizontal resolution simulations using the sixth version of the Canadian Regional Climate Model (CRCM6), operated in convection-permitting mode and developed at the ESCER centre of UQAM, for simulating intense winds and wind gusts. Wind gusts are defined as extreme wind events lasting approximately 3 s, exceeding the mean wind speed by at least 5 m/s. Several CRCM6 configurations are used, with horizontal resolutions of 12, 2.5, and 1 km, all driven by the ERA5 reanalysis. The wind gust diagnostic module, based on the Brasseur method (2001), is activated and diagnoses gusts using turbulent kinetic energy, static stability, and boundary-layer characteristics. The analysis is conducted using two case studies: a synoptic-scale storm that occurred in December 2022 and a mesoscale storm in May 2022, with model results evaluated against observations from meteorological stations across Québec.

For the December 2022 synoptic storm, very high-resolution simulations (2.5 and 1 km) show improved performance in estimating both wind gusts and hourly mean winds compared to the 12 km simulation and the ERA5 reanalysis. Model performance is also generally higher over environments close to water than over land, and under conditions of stronger sustained winds. In contrast, for the May 2022 derecho, the added value of very high-resolution simulations is less systematic than for lower-resolution products, although the 1 km simulation remains the most accurate in representing wind speeds and gusts.

Keywords: Wind gusts, synoptic storm, derecho, mesoscale convective system, high-resolution climate modeling.

INTRODUCTION

Les tempêtes synoptiques ou de mésoéchelle, responsables des vents extrêmes et des rafales de vent intenses, se produisent régulièrement sur le territoire du Québec ou ailleurs dans le monde, et causent des dommages environnementaux, sociaux et économiques importants. Dans le contexte des changements climatiques, les événements extrêmes, dont ceux issus des tempêtes d'origine convective, risquent de devenir plus fréquents et intenses selon les experts du GIEC (Groupe d'experts intergouvernemental sur l'évolution du climat) à l'échelle planétaire (IPCC, 2023 ; Gliksman et al., 2023). Lors de l'occurrence de ces tempêtes, les vents sont responsables de la majeure partie des dommages sur les infrastructures et l'environnement naturel (Hadavi et al., 2022), notamment en raison des rafales dont les vitesses et la direction peuvent changer brusquement dans le temps et dans l'espace. Ceci est à l'origine de déracinements des arbres ou de bris d'infrastructures, comme le réseau de distribution d'électricité. Les rafales se produisent souvent à haute fréquence, entre 3 et 20 secondes, avec une vitesse du vent qui surpasse 5 m/s de la vitesse continue ou régulière (WMO, 2010). Lors d'une tempête, plusieurs facteurs peuvent favoriser des changements dans la direction et la vitesse des vents, notamment les gradients de pression dans le plan horizontal et le cisaillement du vent dans la verticale qui peuvent engendrer des mouvements subsidents (ou *downdraft*) associés le plus souvent à une perte de flottabilité des parcelles d'air (Gliksman et al., 2023).

Au Canada, le Québec est particulièrement vulnérable à l'occurrence des tempêtes comportant des vents et des rafales intenses, en raison notamment de son vaste réseau de distribution d'électricité et de son exposition régulière aux systèmes dépressionnaires synoptiques parmi les plus intenses au pays (cf. durant la saison hivernale dans l'étude de Poan et al., 2018). La moitié de tous ces événements au Canada sont répertoriés au Québec et en Ontario (Hadavi et al., 2022). La présence des Grands Lacs contribue de manière importante à la formation d'événements dommageables qui traversent les deux provinces. Depuis 2000, les tempêtes de vent répertoriées sont en hausse dans cette région (Munoz & Anyomi, 2025). Au Québec seulement, les trois quarts des événements dommageables sont dus aux vents intenses lors de ces tempêtes qui ont causé 1,4 milliard de pertes de biens assurés de 2008 à 2021 (Hadavi et al., 2022).

Bien anticiper les vents les plus intenses lors d'une tempête peut s'avérer très utile afin de réduire les risques pour les populations et les infrastructures face à ce type d'aléa. Cependant, les vents, plus précisément les rafales, résultent de processus atmosphériques complexes et de nature souvent stochastique. Cette variable météorologique fait donc l'objet d'études moins systématiquement. Les analyses sont donc moins nombreuses sur ce sujet, notamment au Canada et au Québec. De plus, la variabilité locale du vent pose d'importants problèmes d'analyse, en raison de nombreux effets locaux qui influencent ses caractéristiques (exemple : topographie, présence de masses d'eau).

Pour améliorer la compréhension des vents, les modèles météorologiques et climatiques sont des outils pertinents pour étudier leur évolution sur le territoire. Cependant, la simulation des rafales avec ces modèles reste un défi, et l'implémentation de méthode d'estimation supplémentaire sous forme de méthode de *post-processing* permet d'en améliorer la compréhension et les résultats obtenus (Brasseur, 2001).

Afin d'étudier les rafales de vent, on doit prendre en compte les caractéristiques des types des tempêtes, et leurs effets sur les vents continus ainsi que les variables qui influencent leur variabilité spatio-temporelle. Les méthodes qui permettent de comprendre et d'analyser les vents intenses et les rafales ont évolué en tenant compte des processus qui se produisent dans la couche limite, la convection profonde et selon le profil de cisaillement (Bradbury et al., 1994 ; Nakamura et al., 1996). Une des premières méthodes proposées pour l'estimation des rafales de vent fut développée par Brasseur (2001), qui inclut une compréhension plus complète des processus impliqués. Par ailleurs, l'effet de la résolution des modèles météorologiques ou climatiques utilisés est un facteur important à considérer dans la simulation adéquate des vitesses et des directions de vents, en particulier les rafales où les vents les plus intenses dépendent entre autres de la présence de reliefs/vallées et de masses d'eau qui est mieux représentée à haute résolution (cf. Goyette et al., 2003 ; Gachon et Saucier, 2002 ; Cholette et al., 2015).

L'analyse de ces processus dans ce mémoire est faite à l'aide d'étude de cas. Nous avons sélectionné deux études de cas représentatives des tempêtes récentes qui ont causé d'importants dommages. Elles font partie des événements qui ont causé le plus de dégât sur le territoire depuis 2000. Le premier cas est celui de décembre 2022, une tempête synoptique hivernale qui incluait des vents forts durant quelques jours. Le deuxième cas est celui de mai 2022, un derecho de mésoéchelle, une tempête rapide qui a causé une quantité de dommages équivalents à la tempête synoptique sur une période plus courte.

Ce mémoire est structuré en trois chapitres. Le chapitre 1 présente la problématique, l'état des connaissances et les objectifs de l'étude. Le chapitre 2 est rédigé sous forme d'un article scientifique qui présente les résultats des simulations à plusieurs résolutions, de deux études de cas (tempête synoptique et de mésoéchelle). Enfin, le dernier chapitre présente une discussion et une conclusion générale.

CHAPITRE 1

Problématique, état des connaissances et objectifs de l'étude

1.1 Impact des vents et des rafales

1.1.1 Variabilité historique

Le vent est une variable cruciale dans l'étude de la variabilité du climat, puisqu'il est responsable de plusieurs processus et modifications des conditions de surface, notamment le transfert de chaleur, d'humidité et d'énergie entre la surface terrestre et l'atmosphère (Jeong et Sushama, 2019 ; Minola, 2020). Par ailleurs au sein de l'atmosphère, les caractéristiques du vent dans l'horizontal et dans la verticale, notamment le cisaillement de celui-ci, dépendent principalement des différences de pression dans l'espace (Sahin et Türkeş, 2013), à la fois près de la surface et dans l'atmosphère (couche limite et atmosphère libre). Le vent est aussi une source de grande incertitude et de préoccupations dans l'évolution du climat, puisqu'il est très variable à l'échelle spatiale et temporelle, et il peut causer d'importants dommages. De manière globale, les tempêtes qui engendrent des vents intenses sont parmi les plus fréquentes et les plus couteuses (Hadavi et al., 2022). Les vents extrêmes et les rafales associées entraînent des dommages sur les infrastructures, mais aussi la végétation et le secteur énergétique (Steinheuer et Friederichs, 2020).

De manière globale les vents moyens sont en constante évolution. Par exemple, on a pu observer une diminution à l'échelle globale des vents moyens dans les années 2000 (Roderick et al., 2007). Cependant, on remarque un renversement de cette tendance depuis 2013 (Azorin-Molina, 2017, 2022). Les causes de ces tendances restent incertaines et plusieurs facteurs pourraient en être responsables, tels que le changement rapide de l'utilisation du territoire et les modifications de la circulation atmosphérique à grande échelle. À l'échelle globale., on observe une diminution de −0,08 ± 0,01 m/s par décennie à une augmentation de 0,24 ± 0,03 m/s par décennie depuis 2010 (Zeng et al., 2019).

1.1.2 Évolution des vents et changements futurs

Au Canada, les vents intenses continus sont principalement dus au cyclone extratropical et aux tempêtes convectives. Dans le futur, un changement dans la fréquence, l'intensité, l'occurrence et la durée des événements causant les vents extrêmes est anticipé (Minola et al., 2020 ; Pryor & Barthelmie, 2010).

Cependant, les régimes de rafales de vent ne suivent pas les mêmes tendances que les vents continus sous l'effet des changements climatiques (Azorin-Molina, 2017, 2022). La fréquence est principalement dictée par l'augmentation des tempêtes extrêmes à travers le globe. De plus, la présence de vents continus extrêmes lors d'une tempête indique également une augmentation des rafales. Les changements dans le régime des vents sont donc d'intérêt dans le contexte des changements climatiques, puisque le vent influence plusieurs secteurs, tels que l'énergie renouvelable, les industries minières et le transport (Cheng et al., 2012 ; Cheng et al., 2014).

1.1.3 Importance de la haute résolution

Les rafales de vent sont par définition hétérogènes ou de nature stochastique dans le temps et dans l'espace, et leur occurrence varie selon les processus ou phénomènes météorologiques impliqués. Les rafales peuvent être estimées de deux manières différentes, soit par une méthode statistique ou soit physique. Les méthodes physiques sont préférables puisque les statistiques assument des conditions stationnaires ou sans contraintes physiques évolutives (Ma et al., 2022). Par ailleurs, plusieurs études ont montré l'importance d'utiliser des modèles physiques ou météorologiques avec une résolution assez fine, puisque les vents sont fortement influencés par la topographie et les conditions de surface à fine échelle (Kurbatova et al, 2018). En effet, la haute résolution permet de mieux représenter les conditions de surface où les rafales se produisent ainsi que les phénomènes atmosphériques, comme les courants aériens descendants (*downdraft*), qui sont influencés par ces effets locaux (Gliksman et al, 2023).

1.2 Théorie et observation des vents et rafales

1.2.1 Processus physique

Brasseur (2001) a établi une méthode d'estimation des rafales de vent (WGE) qui a permis de mieux comprendre les vents, puisque celui-ci est basé sur la physique atmosphérique plutôt que les statistiques. L'étude de Brasseur (2001) a permis de développer et améliorer la méthode WGE ainsi que d'autres méthodes d'estimation des rafales basées sur les principes physiques. Cette méthode est incluse dans le modèle climatique MRCC6 (Modèle régional canadien du Climat version 6) qui est utilisé pour les simulations régionales climatiques à l'échelle du Québec et du Canada produites dans la présente étude.

La modélisation de rafales de vent par Brasseur (2001) est basée sur une compréhension physique du phénomène. Les rafales de vent sont des événements de turbulence non stationnaire qui se produisent donc de manière aléatoire (Boettcher et al., 2003). Elles sont une manifestation de la turbulence dans la couche limite causée par un fort cisaillement vertical et une stabilité statique faible (Ágústsson et Ólafsson, 2009), la stabilité statique représentant la résistance gravitationnelle de l'atmosphère au déplacement vertical (Young, 2014). Dans la verticale, la gravité et le gradient de pression sont le plus souvent en équilibre hydrostatique à grande échelle. La perte d'équilibre hydrostatique représente l'accélération verticale causée par la perte de flottabilité. Cette turbulence permet de générer l'énergie nécessaire pour transférer de la quantité de mouvement grâce aux cisaillements du vent au sein de la colonne d'air ainsi qu'en fonction de la stabilité statique (Stucki et al., 2016). Lorsque le cisaillement du vent est trop intense, les rafales peuvent être déviées avant d'atteindre la surface (Bradbury et al., 1994). Les rafales de vent se forment dans la couche limite où une turbulence dans la colonne d'air surmonte la flottabilité avec une force dynamique vers la surface (cf. schéma présenté à l'Annexe A). Selon Brasseur (2001), cette relation est décrite de la manière suivante :

$$\frac{1}{z_p}\int_0^{z_p} E(z)\,dz \geq \int_0^{z_p} g\,\frac{\Delta\theta_v(z)}{\Theta_v(z)}\,dz \qquad (1.1)$$

Où z_p est la hauteur de la parcelle d'air étudié, g est la gravité, $\Theta_v(z)$ est la température virtuelle potentielle, et $\Delta\theta_v(z)$ est la variation de température virtuelle potentielle dans une couche donnée. Dans l'équation 1.1, $E(z)$ représente le potentiel de flottabilité. (Brasseur, 2001 ; Lu et al., 2022).

De plus, les paramètres locaux de la couche limite exercent une influence plus prononcée sur la vitesse des rafales de vent que les caractéristiques de surface, comme un terrain avec ou sans bâtiments. En effet, le vent moyen est influencé par les changements de rugosité de surface, mais le maximum de vents reste inchangé (Brasseur, 2001). Ce sont pourtant ces caractéristiques de surface qui permettent en partie la formation de la turbulence où la vitesse et l'intensité de celle-ci sont influencées par la taille de l'obstacle. Les caractéristiques de la turbulence et l'intensité sont analysées à l'aide de l'énergie cinétique de turbulence lors d'un événement de vents catabatiques qui se forment près de la mer Adriatique dans l'étude de Večenaj et al. (2010). Cette étude révèle aussi l'importance de bien mesurer les rafales de vent à l'aide d'instruments de mesure appropriés, comme des anémomètres de vents ultrasoniques.

La hauteur de la couche limite atmosphérique affecte également la vitesse maximale des rafales de vent en plus de la topographie. Une couche limite profonde est associée à des vents intenses qui varient également selon la complexité de la topographie (Stucki et al., 2016). Lors d'une rafale de vent, on observe une hausse soudaine de la couche limite (Lu et al., 2022). Ceci est causé par la turbulence associée à la dynamique physique des rafales (Chilson, 2009). Les rafales varient en durée et en intensité selon ces facteurs physiques d'origine dynamique et thermodynamique, et selon le phénomène météorologique concerné. Cependant, l'intensité d'une dépression n'influence pas nécessairement l'intensité des rafales (Mccallum et Norris, 1990).

Dans les tempêtes de mesoéchelle et d'échelle synoptique, les processus dominants et impliqués dans la formation des vents les plus intenses sont différents. De plus, selon le type de tempêtes, les conditions divergent, il est donc difficile d'identifier les causes systémiques des vents intenses (Xiang-E & Xue-Liang, 2012). Par exemple, les rafales descendantes qui proviennent d'orages violents ou de derechos, les vents associés à des dépressions ou les vents descendants et catabatiques causés par la topographie sont affectés par divers mécanismes (Changnon, 2009, 2011). Dans le cas des tempêtes de mésoéchelle, les rafales descendantes sont responsables de la majorité des rafales observées près de la surface (Son et al., 2024 ; Xiang-E & Xue-Liang, 2012), qui sont le plus souvent de très courte durée (Hayashi, 1992).

De plus, les zones qui possèdent un grand potentiel convectif sont les plus susceptibles de générer des rafales (Letson et al., 2018). Ces rafales d'origine convective sont causées par les processus diabatiques et les perturbations thermodynamiques au sein de la colonne d'air (Mohr et al., 2017). Dans une atmosphère instable, les parcelles d'air vont se refroidir et se saturer en eau rapidement lorsqu'elles s'élèvent en altitude. Le développement de précipitations convectives est donc souvent accompagné de rafales (Wakimoto, 2001). Cependant, les rafales non convectives, comme celles associées à des dépressions extratropicales, peuvent être tout aussi dommageables, mais les processus dominants sont très différents (Knox et al., 2011).

1.2.2 Instruments de mesure et modélisation

La mesure et la reconstruction des rafales de vent sont faites soit à l'aide d'instruments de mesure ou des outils de modélisation. Pour les stations d'observations d'Environnement et Changement climatique Canada (ECCC), les mesures sont effectuées à l'aide d'un anémomètre placé à une hauteur de 10 mètres de la surface. Contrairement aux vents (sub-horaires) mesurés de façon continue, les rafales sont mesurées seulement par leur vitesse à fréquence horaire et archivée sur une base quotidienne (Environnement et Changement climatique, Canada, 2023).

Dans les modèles météorologiques et climatiques, les rafales de vent sont simulées à l'aide de méthode variée, soit à l'aide de modèles statistiques, physiques, ou même à l'aide de l'intelligence artificielle ainsi qu'une combinaison de techniques. L'étude de Sheridan (2018) présente et compare les différentes techniques utilisées pour prévoir les rafales de vent, et notamment identifier les méthodes les plus efficaces. Dans le modèle de prévision d'Environnement et Changement climatique Canada (ECCC), la méthode à base physique développée par Brasseur (2001) est utilisée (McTaggart-Cowan et al., 2019). Les simulations réalisées avec ce modèle permettent donc de produire une analyse des rafales de vent en plus de pouvoir les comparer avec les stations d'observation sur le territoire Canadien d'ECCC. Cette approche permet de comprendre et valider les résultats obtenus par la modélisation, comme c'est le cas dans d'autres régions du monde, par exemple, en Europe (Kurbatova et al., 2018).

1.2.3 Application de la méthode de Brasseur : exemples

Comme mentionné précédemment, l'estimation des rafales de vent par la méthode de Brasseur (2001) est basée sur la déviation d'une parcelle d'air par la turbulence dans la couche limite. Pour qu'une rafale de vent atteigne la surface, l'énergie cinétique de la turbulence doit excéder la flottabilité de l'air dans la couche limite. La limite inférieure de l'estimation de la rafale est ainsi déterminée selon la valeur de l'énergie cinétique turbulente locale seulement. La limite supérieure, pour sa part, est déterminée par le vent maximum observé dans la couche limite. L'intervalle d'estimation est finalement influencé par la présence de convection profonde (Bradbury et al., 1994 ; Nakamura et al., 1996). Le module du vent doit considérer la colonne d'air affecté par la rafale descendante. Cette méthode doit être appliquée avec une réanalyse ou un modèle à fine échelle, afin de simuler correctement la convection profonde et donc les rafales de vent associées.

Brasseur (2001) a ainsi produit la première application de cette méthode d'estimation des rafales en analysant des tempêtes de janvier et février 1990 en Belgique. Son étude a utilisé une simulation produite avec le modèle atmosphérique régional (MAR) à mésoéchelle, en utilisant l'analyse ECMWF (European Centre for Medium-Range Weather Forecasts) avec une résolution horizontale de 25 et 50 km. La méthode a permis de reproduire les caractéristiques principales des rafales de vents observés, malgré des cas de surestimation pour les rafales observées d'intensité plus faible. Ces biais sont causés par une mauvaise représentation de la couche limite et du profil vertical de l'atmosphère, la basse résolution de l'analyse utilisée par le modèle et les paramètres de turbulence utilisés dans le modèle (Brasseur, 2001).

Le diagnostic de Brasseur (2001) a été également utilisé dans plusieurs autres études, dans le cadre de l'analyse de rafales de vent en Europe (ex. Goyette et al., 2003). Ces études utilisent souvent des versions modifiées du diagnostic de Brasseur (2001), afin de réduire les erreurs communes, associées à des surestimations des tempêtes intenses (Ágústsson et Ólafsson, 2009 ; Lu et al., 2022 ; Samuelsson et al., 2011). Selon le terrain à l'étude et la résolution utilisée, les résultats et les erreurs diffèrent. Une résolution plus fine permet en général de mieux estimer les rafales et les vents moyens dans les modèles (Ágústsson et Ólafsson, 2009 ; Beluŝić et Klaić, 2004). Lorsqu'un terrain est plus complexe, la résolution est très importante pour obtenir des résultats de bonne qualité. Dans les régions où le terrain est plat, comme celui de la Belgique analysée dans l'étude de Goyette et al. (2003) ou l'Allemagne dans celle de Pinto et al. (2009), la résolution influençait moins la qualité des simulations. Ce résultat est confirmé dans l'étude de Stucki et al. (2016), où la méthode WGE de Brasseur fonctionne mieux dans les plateaux et les terrains moins complexes. Malgré la capacité de la méthode à bien estimer les rafales en terrain montagneux, la méthode de Brasseur (2001) a tendance à sous-estimer les vents dans les pentes descendantes (vents catabatiques) alors que les vents sont surestimés lors de convection intense (Ágústsson et Ólafsson, 2009 ; Born et al., 2012; Lu et al., 2022).

1.3 Lacunes dans les outils de modélisations

Les modèles climatiques régionaux emploient aujourd'hui, avec l'augmentation des puissances de calcul, des échelles horizontale et verticale progressivement plus raffinées dans le but de produire des simulations plus fiables. Cette résolution de plus en plus fine est toutefois associée à des couts de calcul élevés, et n'entraine pas automatiquement des résultats plus précis et une réduction du biais du modèle (Pryor et al., 2012). Dans le cas des rafales de vent, peu d'études ont été réalisées au Canada et au Québec afin d'évaluer la valeur ajoutée de l'utilisation de la très haute résolution, en mode *convection-permitting* (cf. détails dans l'étude au Québec réalisée par Llerena et al., 2023; et Roberge et al., 2024), dans la simulation des vents intenses et des rafales de vent.

1.4 Objectifs de l'étude.

Comme mentionné plus haut, les rafales de vent et les vents les plus intenses sont des variables peu étudiées au Québec. Ce projet s'inscrit dans le projet ARRIMÉ (Aléa, Risques et Résilience des Infrastructures minières et électriques) qui vise à identifier et évaluer les risques reliés aux vents extrêmes pour les infrastructures hydroélectrique et minière. L'objectif principal du présent projet est donc d'analyser la capacité de la 6^{e} génération du modèle régional du climat (MRCC6) développé au centre ESCER à bien reproduire les vents intenses et les rafales dans des cas d'événements spécifiques dommageables pour les infrastructures.

Les objectifs spécifiques sont de :

1. Analyser la valeur ajoutée des simulations à très hautes résolutions (ex. 1 et 2,5 km), en mode convection-*permitting*, versus à plus basse résolution (ex. 12 km), dans la représentation des rafales de vent sur le territoire du Québec à l'aide de la méthode de Brasseur (2001).

2. Analyser la valeur ajoutée du modèle en *convection-permitting* pour la simulation des rafales de vent dans le cas de systèmes convectifs de mésoéchelle versus des dépressions extratropicales d'échelle synoptique.

CHAPITRE 2

Article: Evaluation of wind speeds and gusts as simulated with the CRCM6 regional climate model with convection permitting : Case study of a winter and summer windstorms in southern Quebec

Article à soumettre à Tellus A : Dynamic Meteorology and Oceanography

Amélie Michaud[1], Philippe Gachon[1], Martin Leduc[1,2]

[1] *ESCER (Étude et Simulation du Climat à l'Échelle régionale) centre, Université du Québec à Montréal, Montréal, Québec, Canada;* [2] *Ouranos, Montréal, Canada*

Ce chapitre présente un article préparé pour soumission à la revue Tellus dont le sujet traite de l'analyse de deux études de cas, soit un système convectif de mésoéchelle qui a affecté l'Ontario et le Québec en mai 2022 et une tempête synoptique qui a affecté les mêmes régions en décembre 2022. Ces études de cas permettent d'analyser les simulations du MRCC6 à plusieurs résolutions (12, 2,5 et 1 km) et d'évaluer les vents et les rafales de vents simulés versus celles issues des stations d'observation d'ECCC durant la période où ces deux systèmes météorologiques furent présents au Québec.

Résumé : Les rafales et les vents intenses représentent une des causes principales des dommages et pannes du réseau de distribution d'électricité d'Hydro-Québec lors de tempêtes parfois extrêmes. Cette étude évalue la valeur ajoutée de la très haute résolution spatiale du modèle régional canadien du climat MRCC6, en mode *convection-permitting,* développée au centre ESCER de l'UQAM. Les rafales sont définies comme des épisodes de vents d'une durée d'environ 3 s, dont la vitesse excède les vents moyens d'au moins 5 m/s. Des simulations du MRCC6 à des résolutions horizontales de 12, 2,5 et 1 km, toutes pilotées par la réanalyse ERA5, sont analysées. Le module de rafales de vent est basé sur la méthode de Brasseur. L'évaluation repose sur deux études de cas : une tempête synoptique survenue en décembre 2022 et un derecho de mésoéchelle en mai 2022. Les résultats montrent que, pour la tempête synoptique, les simulations à très haute résolution offrent une amélioration notable de l'estimation des vents horaires et des rafales par rapport à la simulation à 12 km et à la réanalyse ERA5. En revanche, pour le derecho, la valeur ajoutée des simulations à très haute résolution est moins systématique, bien que la simulation à 1 km demeure plus performante par rapport aux autres simulations et aux vents observés.

Abstract: Wind gusts and intense winds are among the primary causes of damage and outages in Hydro-Québec's electricity distribution network during extreme weather events. This study assesses the added value of very high spatial resolution simulations using the Canadian Regional Climate Model, version 6 (CRCM6), in convection-permitting mode, developed at the ESCER Center of UQAM. Wind gusts are defined as extreme wind episodes lasting approximately 3 s, with speeds exceeding the mean wind by at least 5 m/s. CRCM6 simulations at horizontal resolutions of 12, 2.5, and 1 km, all driven by the ERA5 reanalysis, are analyzed. Wind gusts are diagnosed using a gust parameterization based on the Brasseur method. The evaluation is conducted using two case studies: a synoptic-scale storm that occurred in December 2022 and a mesoscale derecho event in May 2022. The results show that, for the synoptic storm, very high-resolution simulations significantly improve the estimation of hourly winds and wind gusts compared to the 12 km simulation and the ERA5 reanalysis. In contrast, for the derecho event, the added value of very high-resolution simulations is less systematic, although the 1 km simulation remains the most skillful.

2.1 Introduction

Extreme wind events from both synoptic and mesoscale storms can lead to major and severe damages to natural and human systems. In the recent decades, many mesoscale and synoptic windstorms in eastern Canada have resulted in significant disruptions to the transportation, electricity and communication systems as well as the environment (Steinheuer & Friederichs, 2020). High-wind events are destructive meteorological hazards, contributing to economic losses associated with storms in Ontario and Québec provinces (Hadavi et al., 2022). In the future, a substantial increase is expected in the frequency, intensity and occurrence of these events (Minola et al., 2020; Pryor & Barthelmie, 2010). However, the links between the changing climate and high wind events are weak (Azorin-Molina, 2017 and 2022), since one needs to consider the type of weather systems, from synoptic (i.e., tropical and extratropical cyclones) to mesoscale convective systems (MCSs; Catto & Dowdy, 2021; Schumacher & Rasmussen, 2020). In particular, the projection of MCSs and their associated hazards remains a major challenge, which results from multiscale processes and insufficient resolution of atmospheric models (Schumacher & Rasmussen, 2020). However, potential improvements in simulated high-wind events and their extreme behaviours using high-resolution convection-permitting models are promising (Cholette et al., 2015; Gutowski et al., 2020; Lucas-Picher et al., 2021; Moreno-Ibanez et al., 2023). There is an increased need for accurate short-and long-term wind simulations associated with severe storms on both local and regional scales to improve preparedness and reduce impacts.

During storms, gusts are the most destructive form of wind as they are characterized by bursts of a minimum of 3 s of winds that exceed the sustained wind (Kolendowicz et al., 2016). They result from nonstationary turbulence occurring randomly in time and space (Boettcher et al., 2003; Drazin, 2002). Gusts are a manifestation of turbulence in the boundary layer caused by intense vertical wind shear and low static stability (Ágústsson & Ólafsson, 2009). Static stability represents the gravitational resistance to vertical movements in storms (Young, 2014). Gusts form in the planetary boundary layer (PBL) when turbulent kinetic energy (TKE) exceeds the buoyancy of an air parcel, allowing dynamic downward momentum transfer toward the surface. In fact, TKE is associated with the generation of eddies within the PBL that may potentially transport momentum from a certain level in the atmosphere down to the surface (Hayashi, 1992). It is thus the essential source for gusts close to the surface (see Goyette et al., 2003).

Another challenging aspect in the simulation of wind gusts remains, such as their high temporal and spatial variability that need to be resolved using high resolution modeling tools (Goyette et al., 2003). Furthermore, the weak correlation between sustained wind speeds and gust magnitudes renders it infeasible to accurately predict gusts based solely on sustained wind measurements (Brasseur, 2001). Research on wind gusts are also limited because these variables fluctuates in less predictable ways than temperature or precipitation ones (Pryor et al., 2012; Turner et al., 2019), i.e. winds are more stochastic by nature than other meteorological variables as they are also strongly affected by local surface conditions and physiographic features as for example the topography (see Goyette et al., 2003) and surface diabatic fluxes, especially over and near water masses or sea-ice margin (see Gachon et al., 2003; Barthelmie et al., 2010; Moreno-Ibanez et al., 2023). In Canada, the observations of wind gusts are very sparse and often temporally incomplete, complicating the analysis of their potential changes across the years and ecosystems (Cheng et al., 2012).

High-resolution regional climate models serve as a valuable tool to study and simulate high wind events and provide more often a better representation of their spatial and temporal variability than coarse scale global climate models, especially for extreme wind speeds and their evaluation under climate change (see Morris et al., 2024). In terms of gusts estimation techniques, these generally fall into two broad categories. The first being a statistical method which uses distribution functions with extreme value theory to predict the winds (Sheridan, 2018). The second type consists of physics-based approaches such as the wind gust estimate method (WGE) proposed by Brasseur (2001) which relies on a parameterization of the PBL physical component. The WGE method is based on the deflection of an air parcel by turbulence in the PBL. The accuracy of the estimation is also influenced by the deepening of the convection during an event (Bradbury et al., 1994; Nakamura et al., 1996). The WGE method is widely used in climate modeling for its ability to provide accurate and consistent results (see Goyette et al., 2003). The application of this method can result in better results and a better understanding of wind gusts (Sheridan, 2018).

In the Quebec region, limited studies have been conducted on the wind gusts involving physically based models that evaluate the accuracy of the WGE method over complex terrain (Cheng et al., 2012; Cheng et al., 2014; Jeong & Sushama, 2019). The heterogeneous regional physiographic feature of the region requires a high-resolution model because wind is highly sensitive to changes in the surface conditions (see Gachon and Saucier, 2003) and within the St. Lawrence valley (see Cholette et al., 2015). Also, the wind behavior fluctuates greatly on intra-annual scale, especially over water masses and oceanic areas, in particular over cold water in summer or sea-ice free areas during winter (see Gachon et al., 2003; Gachon and Saucier, 2003; Moreno-Ibanez et al., 2023), as well as mountainous terrain, valleys and flat land with respect to the occurrence and characteristics of extratropical cyclones and MCSs.

The WGE method is embedded in the sixth generation of the Canadian Regional Climate Model (CRCM6) and permits the simulation of wind during convective events with high-resolution. The CRCM6, developed at the ESCER center (UQAM), is based on the fifth generation Global Environmental Multiscale (GEM5; Girard et al., 2014; McTaggart-Cowan et al., 2019) forecast model developed by Environment and Climate Change Canada (ECCC). This new CRCM6 model (see Roberge et al., 2024; Llerena et al., 2023) uses the atmospheric component of the version 5.1.1 of the GEM5 model (McTaggart-Cowan et al., 2019). The use of this CRCM6 model facilitates the analysis of hindcast high-wind events to determine the accuracy of the model, before using it to evaluate these events under climate change.

This study aims to fill gaps in the existing knowledge on high winds and gusts using CRCM6 initialized and driven at its lateral boundaries by the ERA5 reanalysis developed by the European Centre for Medium-Range Weather Forecasts (ECMWF) (Hersbach et al., 2020). Additionally, this study will assess the capacity of the model CRCM6 and the WGE method to estimate intense wind and gusts during two severe storms. This paper will also examine the potential added value of a high-resolution and convection permitting model in improving the prediction of high winds and gusts. This study uses two case studies of 2022 storms which caused major damage. These two events occurred in spring and winter of 2022, at both mesoscale and synoptic scales. The first case is an MCS derecho event occurred in May 2022 which caused over 550 000 customers to lose electric power in the Outaouais, Laurentides, Lanaudière, Mauricie and Capitale-Nationale regions (Hydro-Québec, 2022). The second case study is an extratropical snowstorm occurred in December of 2022 which resulted in outages to more than 550 000 customers across the province, like the derecho, with the regions of Quebec City, Saguenay and Côte-Nord were mostly affected (Hydro-Québec (2), 2022).

2.2 Data and methods

2.2.1 Study region

The two case studies took place in Québec (Canada), more precisely in the southern part of the province (see Figures 1b and 1c) which represents the region of interest. The area shown in Figures 1b and 1c has a high density of population and a dense network of meteorological stations (presented in the following section with their locations shown in Figure 2a) used here for the comparison with the CRCM6 simulations. The density of population and infrastructures in Ontario and Québec amplifies the damage and socio-economic exposure due to severe meteorological events.

This area is mostly centered around the St. Lawrence River with the Appalachian Mountains in the southeast and eastern sides and the Laurentian and Charlevoix mountainous regions, this valley is a corridor known for strong wind during storm events along the St. Lawrence River towards the Gulf area (Hundecha et al., 2008; Cholette et al., 2015). As shown in Figure 1 (panels b and c), the areas with the highest elevations reach around 1,629 m in the Adirondack Mountains and 1,048 m in the Charlevoix Mountains. In winter, the differences in temperatures between open water and land surface, as well as strong surface diabatic fluxes over open water during cold air advection, results in the development of strong winds over the coastal area and the Gulf of St. Lawrence (see Gachon and Saucier, 2003). The complex terrain and the geography of the region contribute to the development of deep convection during summer months that promotes higher local winds and severe gusts across various areas in eastern North America (Changnon, 2009 and 2011; Letson et al., 2018).

2.2.2 Environment and Climate Change Canada wind observations

Surface wind observation data from Environment and Climate Change Canada (ECCC) serve as a reference for comparing the model simulation (see the model configuration in section 2.2.3). 100 stations were used across the province of southern Quebec with hourly and daily surface observations for the overall analysis (see their locations in Figure 2a). Wind measurement protocols vary significantly across Canada, particularly regarding anemometer position and the temporal resolution of mean wind speed recordings (Cheng et al., 2012).

For detailed analysis, two subsets of 16 stations were selected within the main regions of interest for the regional assessments in each case study. The stations are distributed in four (4) different regions, shown in Figures 2b and 2c, for each case study where the storm patterns affect the wind fields. The 16 stations presented in Table 1 were used for model simulation comparison over similar physiographic features (e.g., topographic and land/coastal areas), with consistency of the observed data and the reliability of the instruments. The wind is measured as the hourly mean speed at 10 m along with the direction. For the available wind gusts data, only wind speed is measured and represents the instantaneous peak values observed during the day.

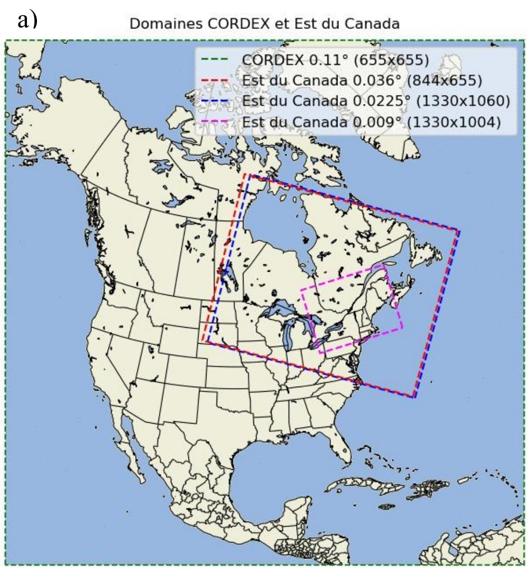

Figure 1. a) Domains of the CRCM6 simulations at three different resolutions: 12 km (CRCM6-12) (in dashed green) covering 655 by 655 grid points, and 2.5 km (CRCM6-2.5) (dashed blue) covering 1330 by 1330 grid points. This is also the domain for the 1 km resolution applied to the 2.5 km grid (CRCM6-1L) covering 3375 by 2700 grid points. Another1 km resolution (CRCM6-1S) (in dashed pink) covers 1330 by 1004 grid points. Panels b and c present orography (in m) over eastern north America with the 2.5 km and 1 km resolution, respectively.

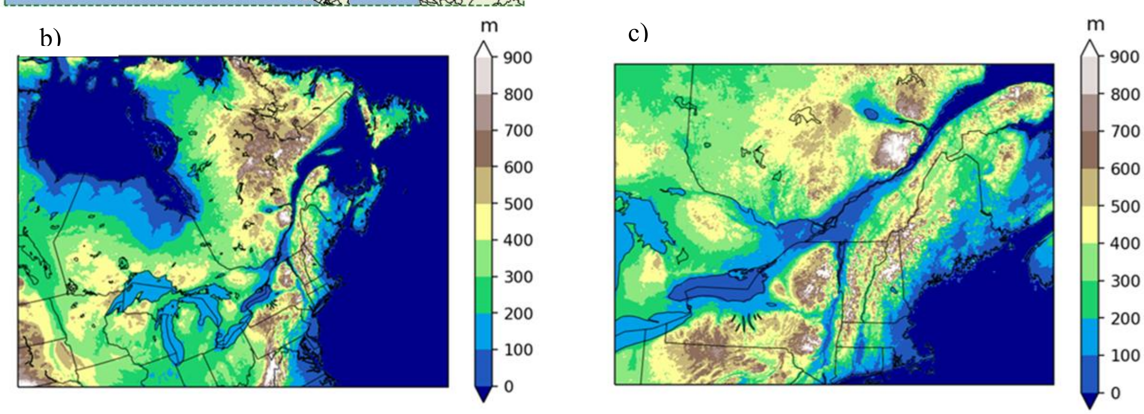

2.2.3 Regional model and reanalysis data

For this study, we used both the CRCM6 and reanalysis data time series of hourly wind values. As suggested previously, the CRCM6 model has been developed by the ESCER (Étude et simulation du climat à l'échelle régionale) Centre at the Université du Québec à Montréal (as described in Llerena et al., 2023; and Roberge et al., 2024). The ERA5 atmospheric reanalysis (Hersbach et al., 2020) served as the initial and lateral boundary conditions for the CRCM6 simulations used in this study. The experimental configuration consists of four simulations, presented in Table 2. The CRCM6 is used with three different resolutions: the coarser resolution is 12 km (CRCM6-12), with the domain covering all North America (dashed green lines in Figure 1a, the 2.5 km resolution grid (CRCM6-2.5) covers the domain of eastern Canada (dashed green lines in Figure 1a, and the 1 km resolution using two different domains, the larger one (CRCM6-1L) and the smaller 1 km domain (CRCM6-1S shown in dashed pink lines in Figure 1a), which includes the southern part of Quebec but excludes the Côte Nord region shown in Figures 2b and 2c, respectively.

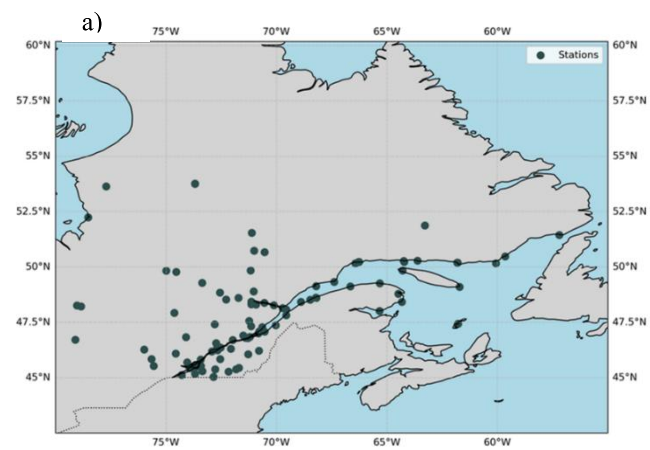

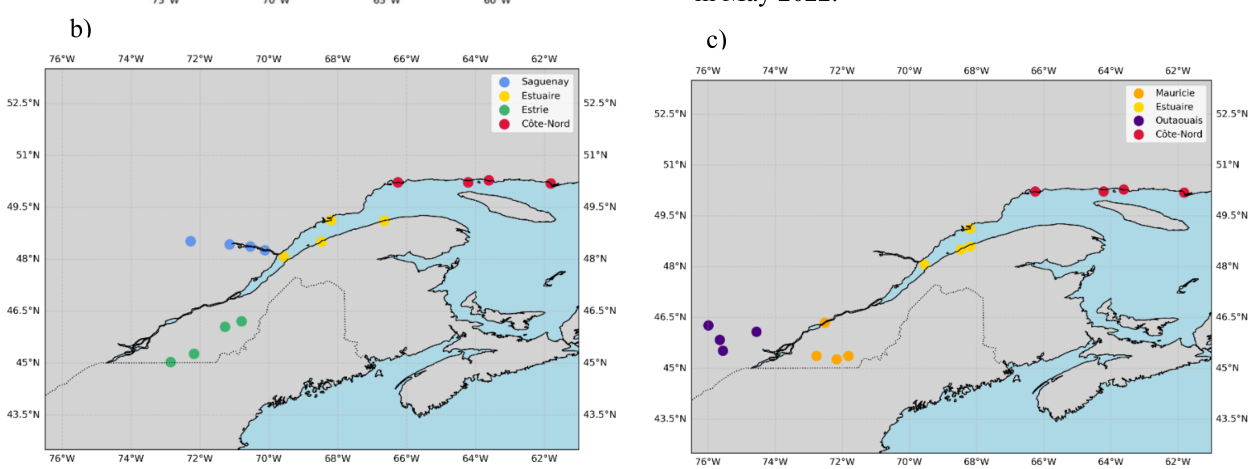

Figure 2. a) Location of the 100 stations from ECCC in Quebec used in the wind analysis of both the December and May 2022 storms. b) and c) Location of the 16 stations from ECCC used for the model comparison for each case study. The stations located in the region of Saguenay are in blue, those in the Estuary (noted as *Estuaire* in the figure) are in yellow, in the Estrie in green, in the Côte-Nord in red. in the Mauricie in orange, and in the Outaouais are in purple. Note that the panel b is used for the case study of December 2022, and the panel c for the case study in May 2022.

For studying the windstorms on a larger scale, the smaller 1 km domain (shown in dashed pink color in Figure 1a) is not used for the stations located in the Côte-Nord regions (red stations located in Figure 1c) as the corresponding simulation (CRCM6-1S) does not cover this area. The main aim of using a larger versus smaller 1 km domain is to evaluate if the size of the domain affects the simulated wind fields, and its accuracy during storm events.

The model configuration includes *convection-permitting* in CRCM6-2.5, CRCM6-1L and CRCM6-1S simulations, i.e. without the parameterization of the deep convection (see Roberge et al., 2024). As shown in the recent work of Ghosh et al. (2025), this configuration is effective to represent deep convection and high intensity of rainfall, with respect to simulation with parameterized deep convection that tends to underestimate precipitation intensity. As suggested in the recent work of Ma et al. (2025), these convective processes simulated with *convection-permitting* model can potentially be useful for the development and evolution of a windstorm or extreme wind events. In general, high-resolution and *convection-permitting* models generally produce more realistic simulations of intense convective events (Belušić & Klaić, 2004; Fosser et al., 2024), as well as for both synoptic (see Ghosh et al., 2025) and mesoscale cyclonic events (see Alpizar et al., 2026)).For the CRCM6-12 simulation, the spectral nudging was utilized to improve the simulation of large-scale patterns during wind events (Separovic et al., 2012; Whittaker et al., 2025). For all simulations (i.e. at 12, 2.5 and 1 km resolutions), ERA5 reanalysis was used as boundary conditions for both atmospheric (temperature and wind fields) and oceanic (sea surface and sea-ice) fields (see details in Table 2).

Table 1. Selected observation stations from ECCC for the analysis of the two storms, i.e. case studies of May (MCS-derecho) and December (synoptic system) 2022 and the location of each of the 16 stations is presented in Figures 2b and 2c, with four stations located in each Côte Nord, Estuary, Saguenay, Estrie or Mauricie, and Outaouais/Laurentides areas.

Stations	Identification number (WMO)	Region	Altitude (m)	Lat (°N)	Lon (°W)	Missing data
Pointe-Claveau	7045398	Saguenay	4.00	48.26	70.11	0 %
Cap-Rouge	7040444	Saguenay	7.30	48.37	70.54	0 %
Jonquière	705S002	Saguenay	135.60	48.43	71.14	0 %
Roberval A	7063370	Saguenay	178.60	48.52	72.27	0 %
Baie-Comeau	7034900	Estuary	68.60	49.13	68.20	0 %
Pointe-au-Père (INRS)	7053KGR	Estuary	7.60	48.51	68.47	0 %
Cap-Chat	7055422	Estuary	36.60	49.11	66.65	0 %
Ile rouge	7042395	Estuary	5.90	48.07	69.56	0 %
Mont-Joli	7053038	Estuary	52.40	48.61	68.19	0 %
Beauceville	7028123	Estrie	160.00	46.21	70.79	0 %
Thetford Mines RCS	7027470	Estrie	310.90	46.05	71.27	0 %
Lac Memphrémagog	7028442	Estrie/Mauricie	208.70	45.27	72.17	0 %
Frelighsburg	701Q009	Estrie	112.80	45.03	72.85	9 %
Sept-Îles	7046059	Côte-Nord	52.60	50.22	66.25	1 %
Ile aux Perroquets	7041JG6	Côte-Nord	9.00	50.22	64.21	0 %
Havre St-Pierre	7041382	Côte-Nord	6.10	50.28	63.61	0 %
Natashquan	7043BP9	Côte-Nord	11.90	50.19	61.81	0 %
Granby	701S001	Mauricie	175.00	45.37	72.77	0 %
Lennoxville	7022579	Mauricie	181.00	45.37	71.82	0 %
Trois-Rivières	7018562	Mauricie	53.30	46.35	72.52	0 %
Ottawa Gatineau	702LED4	Outaouais/Laurentides	64.30	45.52	75.56	10 %
Maniwaki	7032682	Outaouais/Laurentides	199.70	46.27	75.99	0 %
Montréal Mirabel Intl	7032685	Outaouais/Laurentides	82.30	45.68	74.04	0 %
Saint-Jovite	7033121	Outaouais/Laurentides	234.40	46.06	74.56	0 %

Regarding the reanalysis data, ERA5 covers the period from 1950 to the present on a grid resolution of 31 km (Hersbach et al., 2020). It includes hourly archiving of wind field data and gusts (at 10 m). ERA5 was also used in comparison with the CRCM6 data by extracting the hourly wind and wind gust components from the archives for the three-day peak of each storm (see Table 2). The hourly wind speed in the reanalysis was computed from the horizontal wind components U and V. As for the CRCM6 simulations, hourly wind gusts are also used; namely, the variables WGE (wind gust estimate), WGN (wind gust minimum), and WGX (wind gust maximum) were selected. More details on the wind gust estimates are presented in the following section.

Table 2. Model configurations used for the simulation and the characteristics of the different resolution and the variables used. The respective domains of the 12, 2.5, and 1 km CRCM6 resolutions are shown in Figure 1a.

	Simulated Period	Domain	Resolution	Boundary conditions	Period of analysis	Hourly variables	Configuration
CRCM6	15-05-2022 To 31-05-2022 / 20-12-2022 To 31-12-2022	*Eastern Canada (small)*	CRCM6-1S 1 km	ERA5	(Historical) 20-05-2022 To 22-05-2022 / 23-12-2022 To 25-12-2022	*WGN WGE WGX UU VV*	No spectral nudging
		Eastern Canada	CRCM6-1L 1 km CRCM6-2.5 2.5 km				No spectral nudging
		North America	CRCM6-12 12 km				Spectral nudging

2.2.4 Wind Gust Parametrizations

The CRCM6 and the ERA5 reanalysis include a wind gust module based on the WGE method (Brasseur, 2001). The method uses wind gusts as caused by eddies created by the surface friction and wind shear. It determines the location of the eddies and the TKE necessary to overcome the buoyancy of a parcel as described in this equation 2.1:

$$\frac{1}{z_p}\int_0^{z_p} E(z)\,dz \geq \int_0^{z_p} g\,\frac{\Delta\theta_v(z)}{\Theta_v(z)} \qquad (2.1)$$

Where z_p is the height of the air parcel responsible for the gust, *g* is the gravitational acceleration, $\Theta_v(z)$ is the virtual potential temperature, and $\Delta\theta_v(z)$ is the variation of the virtual potential temperature in each layer and E(z) is the TKE computed (Brasseur, 2001; Lu et al., 2022). The WGE method also uses a lower and upper bound to confirm the estimate, the lower bound is determined by the local vertical TKE and the upper bound is determined by the maximum wind in the PBL (Goyette et al., 2003). The interval resulting from the lower and upper bounds is highly influenced by deep convection. The air parcel deviation must consider the air column affected by the downdraft as seen in Brasseur (2001), which uses WGE, WGN and WGX for this purpose.

2.2.5 Analysis method

To analyze the wind data on a common grid, we use conservative interpolation of the U and V variables separately from the lower to the higher resolution grid to transform the data to the smallest grid (the small

1 km grid) using the CRCM6 model simulation without modifying the objects analyzed (Pletzer & Fillmore, 2015). Two domains were also used for the 1km resolution model, CRCM6-1L and CRCM6-1S, to evaluate the effect of the proximity of the lateral boundaries on the simulated winds (i.e. to evaluate the spatial spin-up effect, see Roberge et al., 2024), as well as the effect of large versus small domain on the simulated winds.

Prior to the evaluation of the WGE method over Québec, the analysis of the continuous wind is done. During a convective event, the capacity of CRCM6 to estimate the high continuous speed is important for obtaining an accurate prediction of wing gust (Stucki et al., 2016). The continuous hourly wind speed is a key indicator of the potential performance of the WGE method. This direct comparison of the hourly data available at the station allows for more in-depth analysis. The statistical assessment incorporates 100 stations in higher latitude, and more specific analysis is done on 16 high confidence stations for each event were selected in the targeted area affected by the storm. The nearest grid point for each station is used for the comparison of wind fields. After testing four and more grid points around each station, the simulated wind values are closest to the observed speed with the nearest grid-point values.

For each storm, we use the 100 stations from ECCC as shown in Figure 2a for each of the three days to evaluate the hourly wind speeds along the trajectory of the storms. We used Taylor diagrams (see Taylor, 2001) and Probability Density Function (PDF) estimate (using kernel density estimation, i.e. KDE method, see Węglarczyk, 2018; Soh et al., 2013) to compare observed, reanalysis and simulated wind fields. The Taylor diagram allows to quantify the Pearson correlation, Root-Mean-Square Error (RMSE) and standard deviation between observed and simulated wind values. In each Taylor diagram, a spatial average value is given for each of the three statistical criteria using the grid point values from the CRCM6 simulations close to the 100 stations during the 3 days of the two storm events.

The RMSE statistical criteria is defined as: $RMSE = \sqrt{\frac{1}{N}\sum_{i=1}^{N}(M_i - O_i)^2}$ (2.2)

Where M_i is the model value O_i is the observed value and *N* is the number of paired observations.

The PDF is also constructed using the same 100 stations and model simulated hourly winds using the same three days of both storm events. This will help to determine if the hourly wind speeds are or are not well represented during the 3-days track of each storm.

Another statistical criteria is used to evaluate the accuracy of simulated winds versus the observed ones, such as the Bias that corresponds to the mean difference values between the simulated and the observed wind fields using the 16 stations located in each area presented in Figure 2b and 2c. Therefore, the Skill score (SS) is also used, which allows to calculate the mean squared error between the simulation and the observations using the following equation 2.3.:

$$SS = 1 - \frac{MSE}{MSE_{obs}} \qquad (2.3)$$

MSE is the mean squared error between simulation and observation that allow to quantify the added value from the simulation of peak sustained wind with respect to the sample climatology from observed data MSE_{obs}, which is given here by the average of the squared differences from the mean observation (see further details in Stucki et al., 2016). Positive scores between 0 and 1 mean that the simulation is skillful (von Storch and Zwiers, 2003; Wilks, 2006; Stucki et al., 2016). This yields improvement over the forecasts; a positive score shows an improvement where 1 is a perfect forecast and negative score shows deterioration of the forecast. Relative error was also used in the evaluation of wind gusts to better assess the different results on a comparable scale. Relative error expresses the difference between simulated and observed values as a percentage of the observed value, allowing for a normalized comparison across stations and events with varying wind magnitudes.

2.3 Results

2.3.1 First case study: Extratropical cyclone of December 2022

From 21 to 26 December 2022, an extratropical cyclone brought a significant amount of snow to the northeastern United States, Ontario, and Québec. This storm formed originally in the Canadian Prairies on 21 December (not shown) and reached the province of Ontario on 23 December (see Figure 3a). An occluded front formed north of the center of the cyclone (Chai et al., 2022). Figure 3 illustrates the mean sea-level pressure and wind fields (at 10 m), moving from the Great Lakes on 23 December (Figure 3a) towards Québec (Figure 3b and c) on 24 and 25 December 2022. Precipitation was observed over the Ohio Valley, the Great Lakes, and southern Ontario, turning from rain to snow at 18:00 UTC on 23 December according to station data.

Figure 3a shows the depression on 23 December at 1200 UTC and the associated winds at 10 m where the strongest speeds were in the northeast and east of the storm center in southern Québec and New England states. The wind directions changed with the progression of the front from east to southwest winds (Figures 3a and b). On 24 December, the depression reached the center of the Québec province as shown in Figure 3b. The center of the storm moves toward southeastern Hudson Bay on 25 December with blizzard conditions along the Saint-Lawrence River (Figure 3c; see Chai et al, 2023). The storm declines on the 26 December and fills during its move towards the north of Québec province.

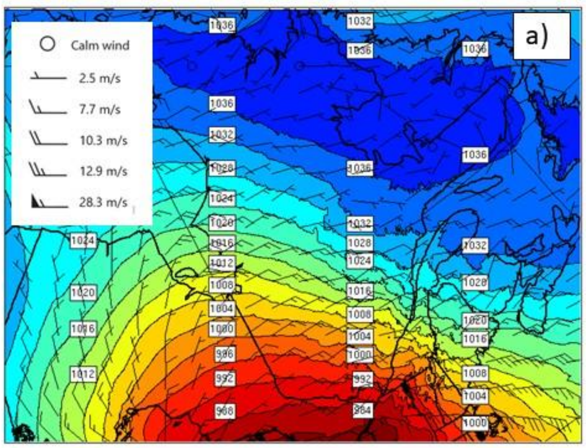

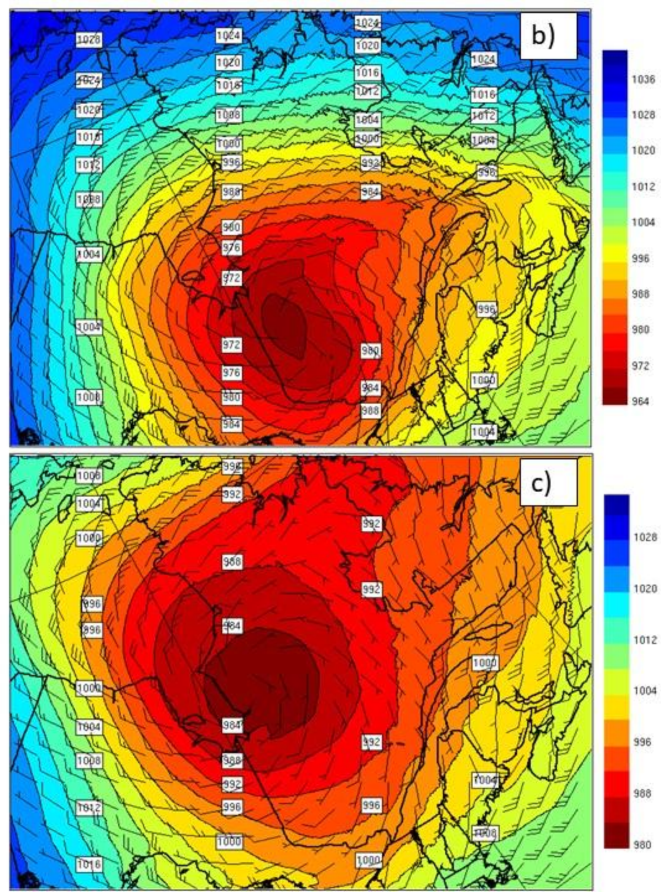

Figure 3. Evolution of the storm over 3 days in December 2022 showing mean sea level pressure (in hPa colour shading, with low pressure in red and high pressure in blue) and winds (in m/s) represented by wind barbs at 10 m on 23 December 12:00UTC (a), 24 December 12:00 UTC (b), and 25 December 12:00UTC (c) using ERA5 reanalysis data.

2.3.2 Hourly wind speeds comparison in Québec during the December storm event

The most intense phase of the storm in Québec occurred between December 23 and 25, as shown in Figure 3, with the highest wind speeds recorded on the south of the province on the 23. The analysis from 100 ECCC stations (see their locations in Figure 2) exhibit varying degrees of accuracy depending on both the day and the model resolution used. Figure 4a shows a Taylor diagram from hourly wind speeds over each day, between 23 and 25 of December 2022, using all datasets from ERA5 and all CRCM6 simulations with respect to the 100 observed stations used as a reference dataset. This diagram includes the mean values of Pearson correlation, centered RMSE and standard deviation (SD) ratio. The higher correlation, lowest RMSE and relatively similar SD ratio among all products versus observed data are obtained on December 23 (Figure 4a), when the low pressure was in southern Québec (as shown in Figure 3). The CRCM6-1S simulation performs slightly better than other simulations and the reanalysis products on that day. On December 24, the correlation computed from hourly wind speeds decreases for all simulations and reanalysis compared to the previous day, as along with the increase in RMSE and a general lower SD of all simulated/reanalysis fields than the observed ones.

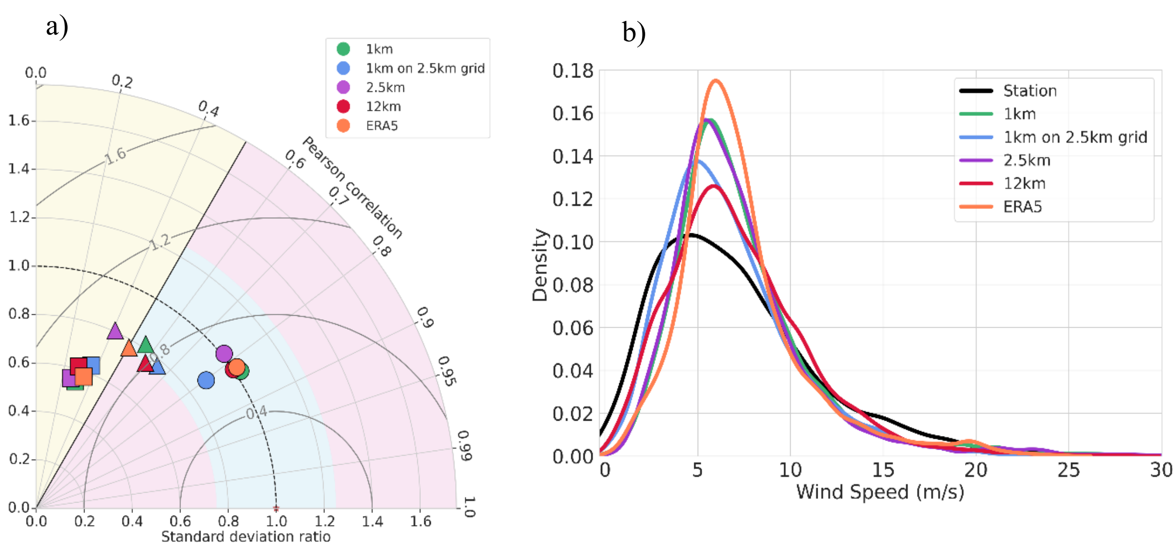

Figure 4. a) Taylor diagram with mean values of Pearson correlation, standard deviation ratio and centered RMSE (solid circle lines) computed for all simulations (CRCM6-12, CRCM6-2.5, CRCM6-1L and CRCM6-1S) and ERA5 reanalysis with respect to the 100 stations hourly wind data used as a reference, for each day between 23 and 25 of December 2022. Circles represent 23 December, triangles represent 24 December and squares represent 25 December 2022. b) Probability density function of hourly wind speed for the 100 stations and the closest values from the simulated and reanalysis data during the three days of the extratropical cyclone present in Québec (as shown in Figure 3). Note that only a subset of 50 stations is used for CRCM6-1S.

This means that the ECCC observations presented higher variability across the Québec province resulting in reduced performance metrics for that day. In such case, the CRCM6-1L simulation presents the best results among all runs. On 25 December, the overall lowest wind speeds from the three days' time series were recorded over southern Québec when the storm moved toward southeastern Hudson Bay. The performance metrics show the lower accuracy among the three days, with correlation between the simulations and ECCC stations varying between 0.2 to 0.4 with no statistically significant values (see Figure 4a). The best statistical scores are obtained on such day with the CRCM6-2.5 simulation. Annex B shows a similar Taylor diagram but only using 16 stations shown in Figure 2, it shows very similar data and the distinction between the three days.

The probability density function (PDF) using the hourly winds from 23 to 25 December 2022 is shown in Figure 4b, using both observations, reanalysis data, and simulated values. The ERA5 reanalysis shows the poorest results and underestimates both low and high wind speed values, resulting in a narrow distribution compared to the station data. The CRCM6-1S and CRCM6-2.5 simulations show a similar distribution and tend to overestimate the presence of low-speed wind with respect to observed data. The CRCM6-1L and CRCM6-12 are quite comparable and more closely match the PDF of the observed stations. Overall, the observed distribution of hourly wind speeds presents higher spatial variability, with a slightly higher occurrence of strong winds compared to the CRCM6 simulations.

2.3.3 Mean and maximum wind speeds in specific regions during the December storm event

Figure 5 shows the comparison of hourly wind speeds over the three days (23–25 December 2022) between all CRCM6 simulations, ERA5 reanalysis, and the observed ECCC stations for three regions and six specific stations from Saguenay, Estuary, and Estrie areas (see their locations in Figure 2b). As suggested previously, the highest wind speeds were observed on the first day (23 December 2022), with peak wind speeds occurring above 15 m/s between 06:00 UTC on 23 December and 06:00 UTC on 24 December over the Saguenay area and the Estuary (see Figures 5a–c). A secondary maximum wind speed was also observed in the mouth of the Saguenay River and the Estuary on 24 December during the whole day (Figure 5d). This resulted in lower wind speeds in the south, over the Estrie region (Figures 5e–f). The CRCM6 simulations at every resolution as well as the ERA5 reanalysis underestimate the hourly wind speeds when wind peaks are observed. This means that the highest winds lead to more underestimation by model runs, whereas lower winds show fewer discrepancies between the observed ECCC data and the CRCM6 simulations in all regions. The simulations accurately follow the observed time series, with the highest wind speeds reached by CRCM6-1S, which is the simulation that is most similar to the observed data, in particular over the Saguenay and Estuary areas. In these areas, the coarser resolution simulation (CRCM6-12) and the ERA5 reanalysis reveal the least accurate wind speed values compared to observed data, with a systematic and stronger underestimation of the highest observed values (Figures 5a–d). The lowest-performing dataset is the ERA5 reanalysis, reaching only 16 m/s compared to the 27 m/s measured at the station over the 23-24 of December. In summary, the higher-resolution simulation using the smaller domain (CRCM6-1S) presents in general the best skill among all regions with respect to observed data.

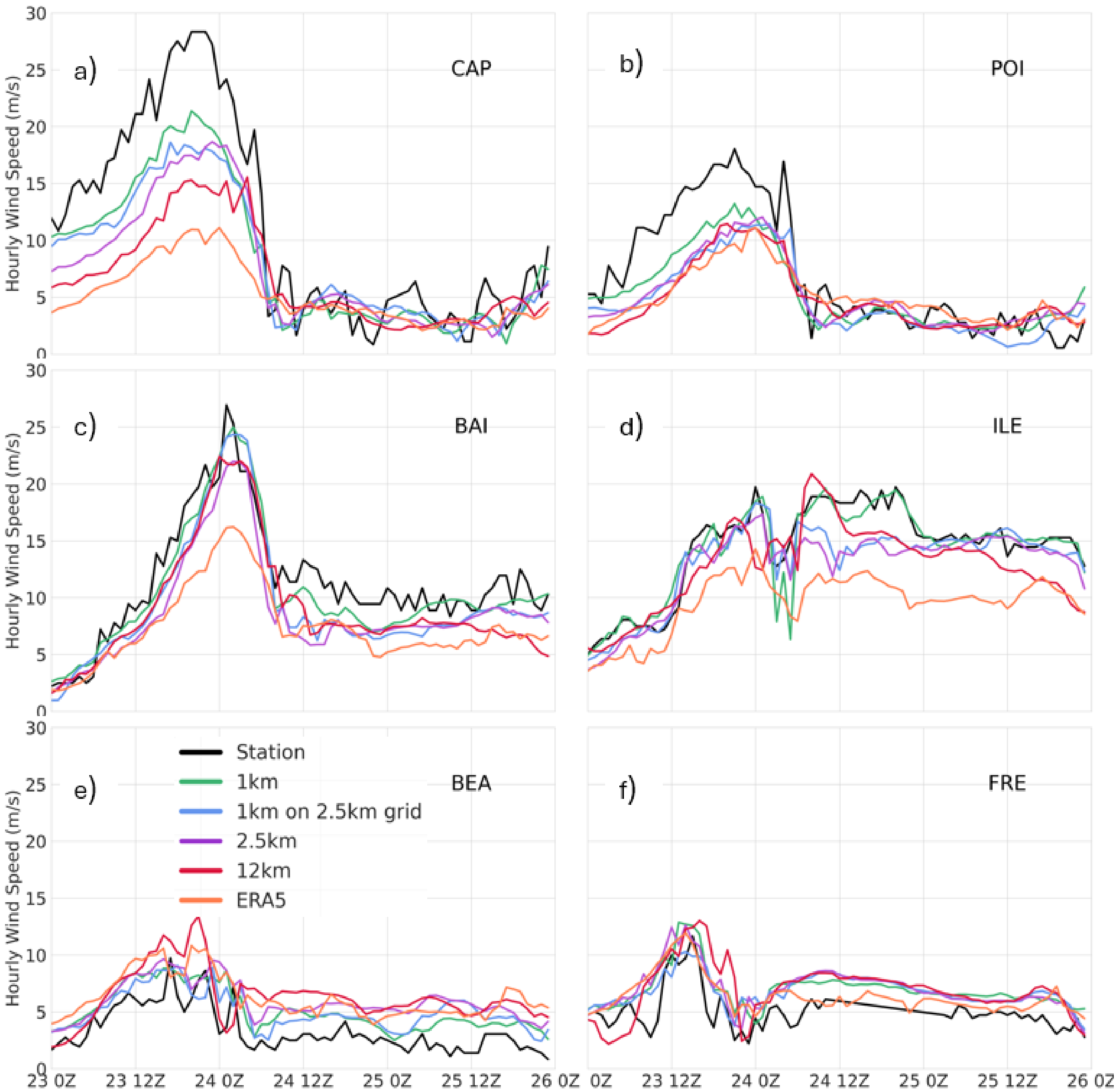

Figure 5. Temporal evolution of hourly wind speeds during the storm event at six specific stations from 00:00 UTC on 23 December to 00:00 UTC on 26 December. The locations are the Saguenay Valley (a and b panels), the Estuary region (c and d panels), and the Estrie region (e and f panels). The station abbreviations are Cap-Rouge (CAP), Pointe-Claveau (POI), Baie-Comeau (BAI), Île Rouge (ILE), Beauceville (BEA), and Freligshsburg (FRE). The black line shows the wind measured at the station, the green line represents CRCM6-1S, the blue line is CRCM6-1L, the purple line is CRCM6-2.5, the red line is CRCM6-12, and ERA5 is shown in orange.

Table 3. Comparison of Pearson correlation (cor), root mean squared error (RMSE), additive bias (BIAS), and skill score (SS) calculated from hourly wind speeds the reduction of variance of all simulated data from CRCM6-1S, CRCM6-1L, CRCM6-2.5, CRCM6-12, as well as ERA5 reanalysis, and the ECCC stations (used as reference) listed in Table 1, using four stations from each region and the mean of all 16 stations. The four regions include Saguenay, Estuary, Estrie and Côte-Nord and their four stations located in each region as shown in Figure 2b. The bold values represent the best results for each statistical criteria and for each simulation or reanalysis among all regions, with blue bold values the best ones among all products.

CRCM6-1S				
	cor	RMSE	BIAS	SS
All	0.84	2.13	**-0.05**	0.63
Saguenay	0.86	2.20	-2.48	0.72
Estuary	**0.87**	2.18	-1.99	**0.75**
Estrie	0.80	**1.55**	4.31	0.43
Côte-Nord	-	-	-	-
CRCM6-1L				
	cor	RMSE	BIAS	SS
All	0.80	2.18	-1.03	0.59
Saguenay	0.82	2.50	-3.59	0.72
Estuary	**0.87**	2.22	-3.81	**0.75**
Estrie	0.73	**1.51**	2.81	0.43
Côte-Nord	0.78	2.48	**0.46**	0.45
CRCM6S-2.5				
	cor	RMSE	BIAS	SS
All	0.75	2.84	**0.26**	0.19
Saguenay	0.81	2.51	-3.74	0.61
Estuary	**0.82**	2.60	-3.73	**0.65**
Estrie	0.67	**1.81**	4.88	0.17
Côte-Nord	0.69	4.44	3.61	-0.67
CRCM6-12				
	cor	RMSE	BIAS	SS
All	0.65	2.85	**0.57**	0.19
Saguenay	0.66	2.95	-2.92	0.42
Estuary	**0.76**	3.12	-3.24	**0.55**
Estrie	0.52	**2.31**	6.22	-0.30
Côte-Nord	0.64	3.01	2.22	0.07
ERA5				
	cor	RMSE	BIAS	SS
All	0.68	2.55	**-0.64**	0.36
Saguenay	0.57	2.97	-4.59	0.27
Estuary	**0.83**	2.80	-4.28	**0.63**
Estrie	0.52	**1.94**	3.78	0.08
Côte-Nord	0.79	2.49	2.53	0.47

Table 3 presents various statistical criteria (Pearson correlation, RMSE, Bias, and Skill Score) with a comparison between all simulated and reanalysis values of wind speeds using observations from stations during the three storm days (from 23 to 25 December 2022 at 00:00 UTC). The highest Pearson correlation among all regions and simulations have been obtained over the Estuary area and with the 1 km resolution (for both small and large grids, i.e., CRCM6-1S/L). This correlation between the stations and CRCM6-1S/L is 0.87 for the Estuary region, decreasing to 0.86 in Saguenay and 0.80 in Estrie. The Skill Score shows higher values for CRCM6-1S and for regions with the strongest winds (0.73 in Saguenay and 0.75 in the Estuary), whereas for the Estrie area, which has the lowest overall winds, it shows a Skill Score of only 0.43. The CRCM6-1S and CRCM6-1L simulations also present the lowest RMSE values among all simulations and reanalysis, with the Estrie region showing the best result for this metric across all simulations. Finally, the bias shows negative values in areas with high winds (Saguenay and Estuary) and positive values in Estrie and Côte-Nord, where wind speeds are generally lower, with the lowest bias values for CRCM6-1S among all runs and regions. In summary, the results indicate the best performance for CRCM6-1S and CRCM6-1L simulations over all regions.

In summary, this winter storm event produced very high sustained winds over two days, with the highest wind speed observed as well as simulated in the Saguenay and Estuary areas. In fact, the strongest winds were concentrated along and near the St. Lawrence River, where the detailed analysis was conducted. Comparisons among all simulations and reanalysis show more often a better agreement with the ECCC station data during the hours of highest wind intensity. The Estuary region shows the best agreement with the station data, and the best results among runs and regions are obtained from the CRCM6-1S and CRCM6-1L simulations (Figures 5a and b and Table 3). In general, the maximum values are underestimated in all simulations, especially in the coarse-scale resolution products (CRCM6-12 as well as the ERA5 reanalysis).

Also, for all CRCM6 simulations, performance improves with higher resolution. The correlation between the simulated and observed datasets also increases with resolution. The performance of CRCM6-1S is the best according to the temporal evolution of the storm (Figure 5) and the related statistics (Table 3). In other words, ERA5 and the CRCM6-12 coarse-resolution simulation perform the worst. In fact, the probability density function shows that ERA5 strongly underestimates wind speeds in most regions. The CRCM6-12 simulation shows the worst statistics in the analysis, where the correlation and Skill Score are the lowest.

2.3.4 Second case study: mesoscale convective system (derecho) of May 2022

The MCS event was a fast-moving derecho system that occurs during less than 12 hours along a 1,000-km track and 100-km wide path (Ashton, 2023). Although the storm was small in scale, it has affected southern

Ontario and Québec, where 40% of the Canadian population lives (Gatzen et al., 2025). The derecho formed south of the Great Lakes following warm temperatures during 19 to 21 of May 2022 (Henson & Masters, 2022). A cold front around 21 May at 12:00 UTC with high wind speeds caused a thunderstorm to form, the storm deepened when it reached the Great Lakes and the thunderstorm formed a bow echo (Ashton, 2023). The derecho that developed over southern Ontario and Québec, was associated with high winds and intense precipitation (not shown) on May 21, mainly between 12:00 and 18:00 UTC (as shown in Figure 6)

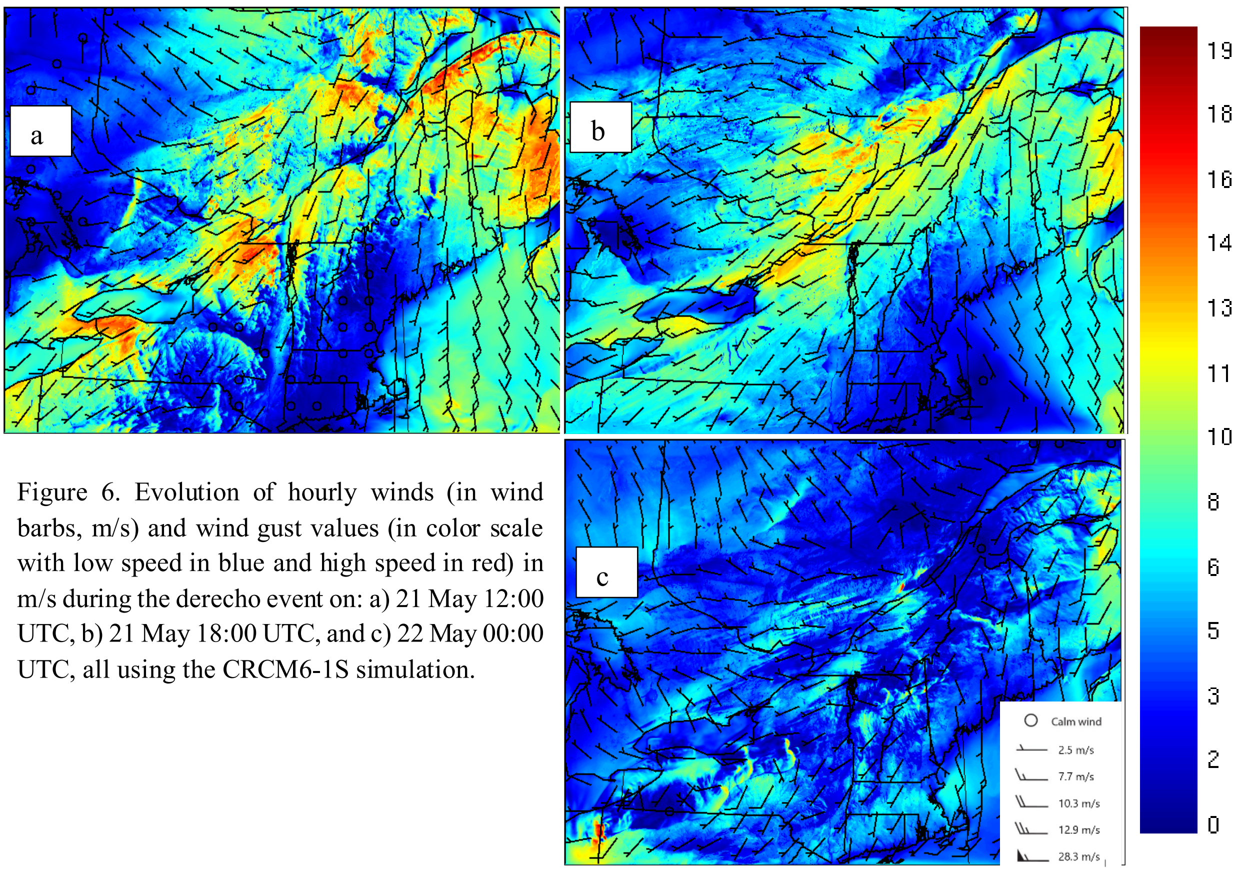

Figure 6. Evolution of hourly winds (in wind barbs, m/s) and wind gust values (in color scale with low speed in blue and high speed in red) in m/s during the derecho event on: a) 21 May 12:00 UTC, b) 21 May 18:00 UTC, and c) 22 May 00:00 UTC, all using the CRCM6-1S simulation.

2.3.5 Hourly wind speeds comparison in Québec during the May storm event

The MCS storm caused significant damages over a short time period (Gatzen et al., 2025) with very intense winds concentrated in a brief interval over the three-day period from 19 May 12:00 UTC and 22 May 12:00 UTC, with the maximum wind speeds occurring between 15:00 UTC on 21 May (see values on 12:00 UTC on 21 May in Figure 6a and 09:00 UTC on 22 May.

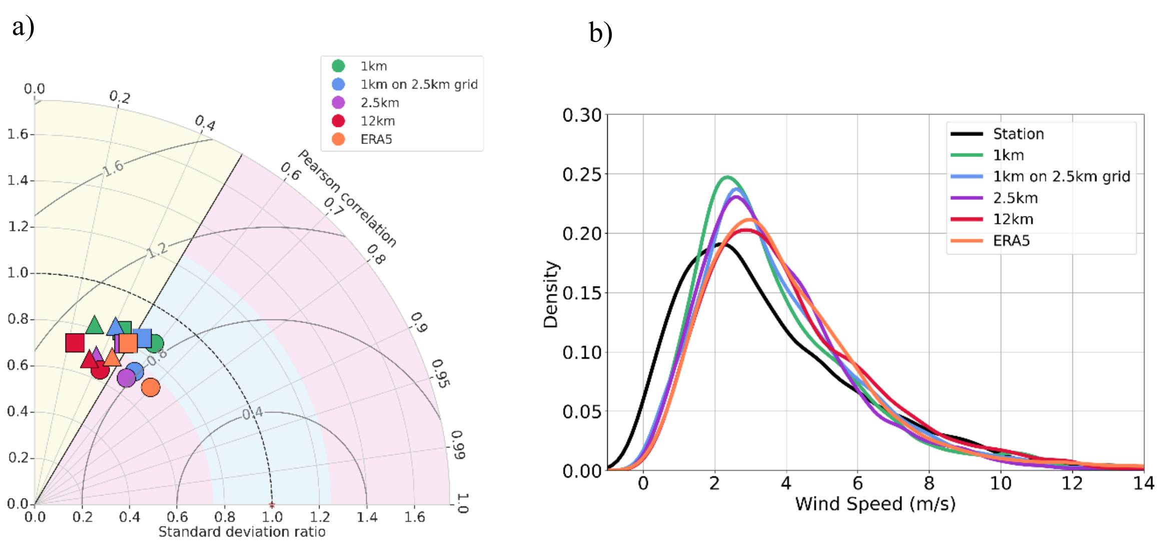

Figure 7. a) and b) Same as Figure 4a and Figure 4b (respectively), but for the derecho storm event (20-22 May 2022). Circles represent 20 May; triangles represent 21 May and squares 22 May.

Figure 7a shows the Taylor diagram over the three days (20–22 May 2022) with quite similar results among the simulations for each day. CRCM6-1S shows the best agreement, with the standard deviation ratio between 0.8 and 1 for each day. For most products, the simulations and reanalysis present a Pearson correlation between 0.2 and 0.7, with the best results from the ERA5 reanalysis, followed by the CRCM6 simulations at 1 and 2.5 km resolution on 20 and 21 May. Quite similar RMSE values are also obtained among all products with respect to observed stations (on average). Annex B shows a similar Taylor diagram but only using the 16 stations shown in Figure 2, it shows very similar data.

As shown in Figure 7b, the PDF of hourly wind speeds shows a heavy tails distribution, but with lower extreme values compared to the synoptic storm analyzed previously (see Figure 4b). The CRCM6-1S shows the best agreement with the observed median values followed by CRCM6-2.5 and the CRCM6-1L, while the CRCM6-12 simulation and the ERA5 reanalysis reveal in general an overestimation of hourly wind speeds in most cases. In summary, as also shown in Figure 7a, although the higher resolution simulations perform the best for lower and median quantiles of hourly wind speeds, it is difficult to distinguish which simulation performs the best for higher quantiles.

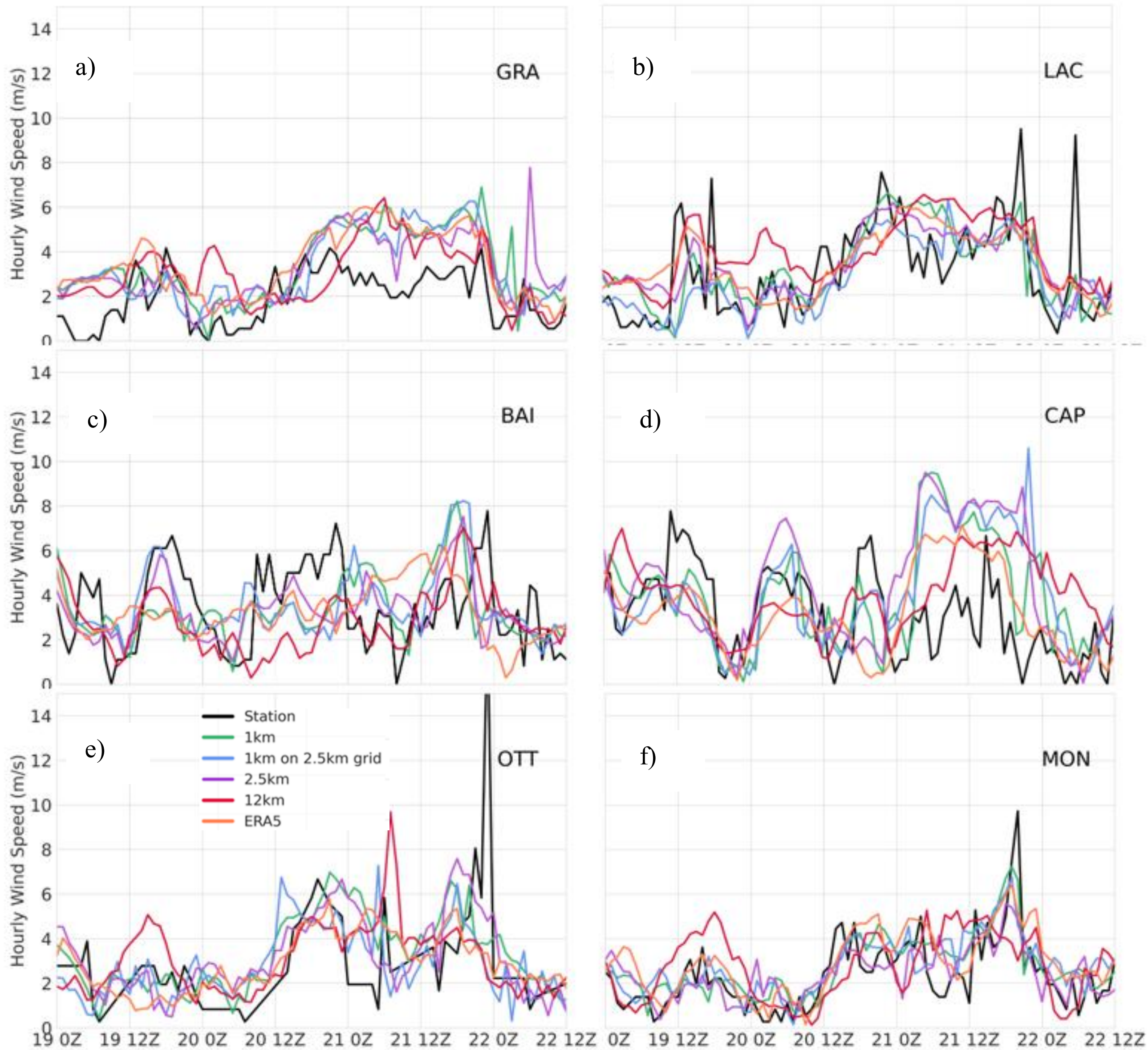

Figure 8. Same as Figure 5 but for the derecho storm event between 00:00 UTC on 19 May to 12:00 UTC on 22 May at six specific locations. The locations are the Estrie region (a and b), the Estuary region (c and d), and the Ottawa/Laurentides region (e and f). The station abbreviations are Granby (GRA), Lac Memphrémagog (LAC), Baie-Comeau (BAI), Cap-Chat (CAP2), Ottawa (OTT), and Mont-Joli (MON). The black line shows the wind measured at the stations, the green line represents CRCM6-1S, the blue line is CRCM6-1L, the purple line is CRCM6-2.5, the red line is CRCM6-12, and ERA5 is shown in orange.

2.3.6 Hourly wind speeds in specific regions during the storm event (20-22 May 2022)

Figure 8 shows the comparison of hourly wind speeds between CRCM6 simulations, ERA5 reanalysis, and observation stations over the three days (19–22 May 2022) and six locations across southern Québec. As revealed in this figure, the high winds occur sporadically at a few locations on May 21 and 22, with values exceeding 8 m/s, whereas the wind gusts were also not sustained for a long period of time. The Ottawa River basin was first hit with the fast-moving storm, which resulted in winds reaching 15 m/s, with a systematic underestimation from all products (CRCM6 simulations and ERA5 reanalysis), as shown in Figure 8e. Examining the Estrie region (Figures 8a and b), the CRCM6 simulations generally follow the temporal distribution of observed data. The CRCM6-1S and CRCM6-2.5 simulations capture the major variations, whereas CRCM6-12 exhibits more inconsistent peaks, including a systematic overestimation in wind speeds with respect to observed values. For the other regions or stations, although the more erratic pattern of wind speed is not fully replicated, the overall fluctuations are well represented in the CRCM6 simulations, in particular with high-resolution simulations (at 1 and 2.5 km). In the Estuary region (Figures 8c and d), the simulations tend to overestimate wind speeds when the stations record small changes, particularly as the storm passes over the eastern area of the Gulf of St. Lawrence (Cap-Chat location shown in Figure 8d). In the Outaouais region, the temporal series is again generally well represented, but the intense peaks measured at the stations on May 21 are not fully captured by all simulations (Figure 8e).

Table 4. Same as Table 3 but for the derecho storm event between 00:00 UTC on 19 May to 12:00 UTC on 22 May over the four regions. The four regions include Mauricie, Estuary, Outaouais and Côte-Nord and their four stations located in each region as shown in Figure 2b. The bold values represent the best results for each simulation or reanalysis among all regions, with blue bold values the best ones among all products.

	CRCM6-1S			
	cor	RMSE	BIAS	SS
All	0.56	**1.50**	0.66	0.09
Mauricie	0.51	1.52	0.70	-0.01
Estuary	**0.59**	1.51	**0.35**	**0.18**
Outaouais	0.59	1.48	0.94	0.10
Côte-Nord	-	-	-	-
	CRCM6-1L			
	cor	RMSE	BIAS	SS
All	0.57	1.44	0.26	0.18
Mauricie	0.51	1.49	0.57	0.02
Estuary	0.61	**1.35**	**0.23**	**0.24**
Outaouais	0.53	1.45	0.73	0.10
Côte-Nord	**0.65**	1.47	-0.50	0.37

CRCM6-2.5				
	cor	RMSE	BIAS	SS
All	0.58	1.51	**0.28**	0.16
Mauricie	0.57	**1.43**	0.61	0.18
Estuary	0.57	1.50	0.39	0.14
Outaouais	0.57	1.54	0.95	0.08
Côte-Nord	**0.61**	1.57	-0.81	**0.25**
CRCM6-12				
	cor	RMSE	BIAS	SS
All	0.51	1.65	0.35	-0.03
Mauricie	0.50	1.68	0.94	-0.08
Estuary	0.46	1.74	**0.13**	-0.16
Outaouais	0.47	1.62	1.08	-0.12
Côte-Nord	**0.60**	**1.58**	-0.76	**0.25**
ERA5				
	cor	RMSE	BIAS	SS
All	0.56	1.51	0.51	0.18
Mauricie	0.52	1.49	0.71	0.10
Estuary	**0.59**	1.53	0.30	0.19
Outaouais	0.49	1.53	0.89	0.03
Côte-Nord	0.64	**1.47**	**0.13**	**0.41**

In Table 4, the overall statistical criteria (Pearson correlation, RMSE, Bias, and Skill Score) with a comparison between all simulated and reanalysis values of wind speeds with respect to observed data reflect, in general, a lower skill of all simulations than for the synoptic low-pressure system, as shown in Table 3. In fact, the best-performing simulation is the CRCM6-1L for the correlation and RMSE criteria, over the Estuary and the Côte-Nord areas. For the Skill Score and mean bias criteria, the ERA5 reanalysis performs best, followed by the CRCM6-12 simulation. Overall, the effect of higher resolution within the CRCM6 simulations is less evident for the derecho event in terms of added value for hourly wind speeds, with respect to the synoptic low-pressure system previously analyzed.

2.3.7 Wind Gust estimates for both storm events

This section focused on the wind gust analysis on both case studies. The WGE method (Brasseur, 2001) uses the continuous hourly wind speed to estimate the minimum (WGN), and maximum (WGX) wind gust values. In this section, we will mainly concentrate on the WGE values per day from all CRCM6 simulations as well as ERA5 reanalysis products to compare those with the observed data, whereas for this last the wind gust speed is measured and represents the instantaneous peak values observed during the day. In the following, a comparison is presented between the observed maximum gust value and the corresponding simulated WGE, as well as the relative error between the simulated and observed values.

2.3.7.1 Maximum wind gusts for the December 2022 synoptic storm event

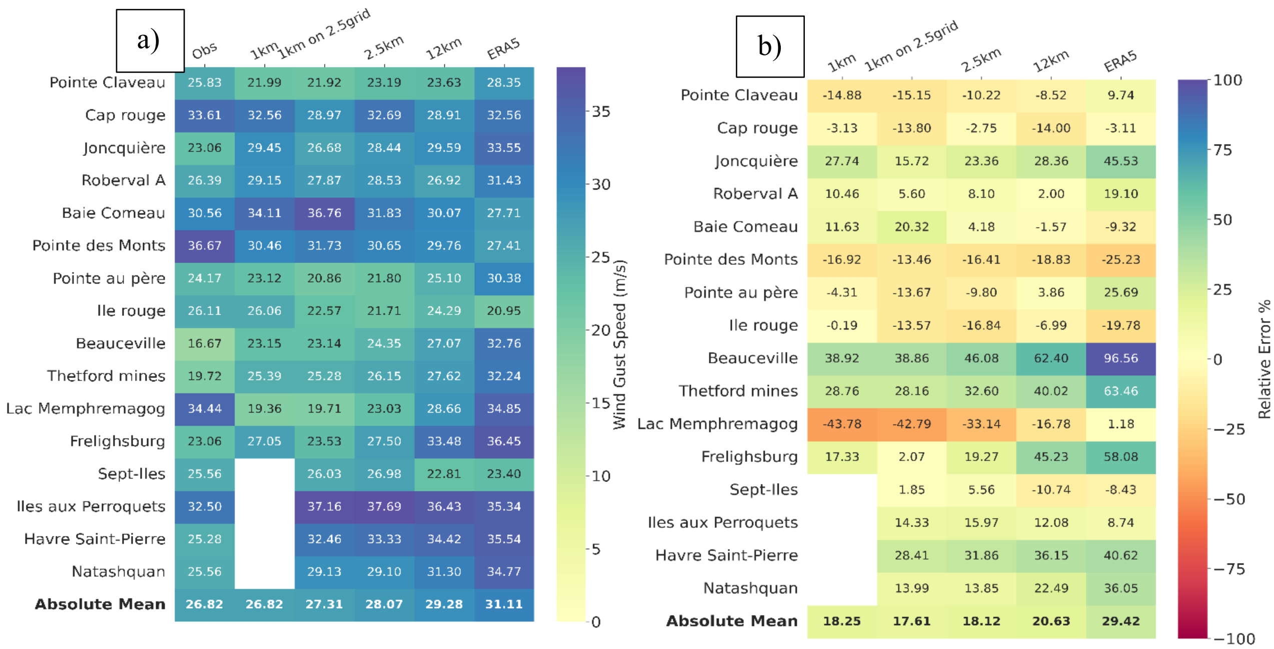

Figure 9. a) Comparison during the storm event from 23 to 25 December of wind gust speeds (WGE) between observations at each station and the CRCM6-1S, CRCM6-1L, CRCM6-2.5, CRCM6-12, and ERA5 (within ±6 hours of the observed time values at each station). b) Relative error (%) of the wind gust speeds (WGE) between observations and each simulation or reanalysis, along with the absolute mean of the relative errors (last row values).

Figure 9 shows the comparison between the simulated and reanalyzed wind gusts (WGE) values and those from observed stations, as well as the relative errors between simulations/reanalysis vs observed products over all locations. These WGE values correspond to the gust observed during the event within ±6 to the simulated values. Figure 9a shows the speed in m/s and Figure 9b is the relative error. The highest wind gusts were observed in the Estuary region (Baie-Comeau, Pointe-des-Monts, Pointe-au-Père, and Île Rouge) and the Côte-Nord region (Sept-Îles, Îles aux Perroquets, Havre-Saint-Pierre, Natashquan), whereas the Saguenay region shows lower values across its four stations (Pointe-Claveau, Cap-Rouge, Jonquière, and Roberval A). The Estrie region (Beauceville, Thetford Mines, Lac Memphrémagog, and Freligshsburg) exhibits in general lower WGE values, except for the Lac Memphrémagog station where the second highest wind gust speed is observed. In most cases, the highest resolutions (CRCM6-1S and CRCM6-1L) provide the closest values with respect to observed wind gusts for the majority of stations, and lowest relative bias except for few stations in the south of Québec (Figures 9a and 9b). In general, for the lowest observed wind gust values, the highest relative errors are obtained from the CRCM6 simulations and reanalysis, with the higher biases up to 96.56% from the ERA5 reanalysis. This last tends to strongly underestimate the values observed where maximum WGEs occur (e.g., Pointe-des-Monts and Île Rouge, see Figure 9b). Other regions and stations with higher wind gusts demonstrate better accuracy among CRCM6 simulations, particularly in the Saguenay, Côte-Nord, and Estuary regions.

2.3.7.2 Maximum wind gusts for the May 2022 derecho event

The measured and simulated wind gusts exhibit considerable variability depending on the location and the strength of the preceding hourly winds, as shown in Figure 10. Observed wind gusts were often very sudden and short-lived, dissipating quickly after onset. Wind gusts differ substantially from hourly winds; for example, at the Lennoxville station, continuous winds were below 9 m/s, while the observed gust reached 24.44 m/s, i.e., 171% higher than hourly values. MCS events like the May derecho are particularly challenging for the model to replicate (see the review of MCSs in Houze, 2018, and the recent work of Alpizar et al., 2026), in particular because MCS forward motion is influenced by three factors: mean wind speed, upwind propagation, and downwind propagation (see Corfidi, 2003); this last factor influences the occurrence of wind gusts.

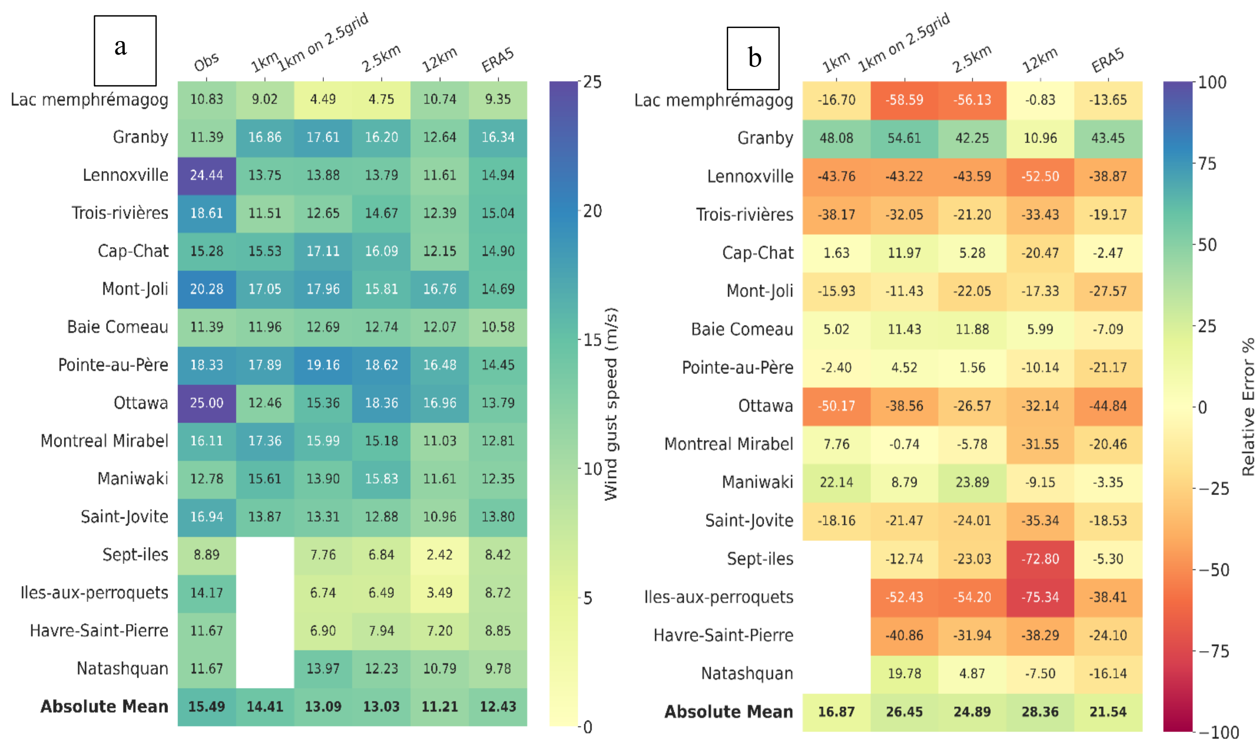

Figure 10. a) b) Same as Figure 9 but for the derecho storm event during the 20 to 22 May period.

For stations with more typical wind gusts, the simulations represent the observations more accurately, though instances of over or underestimation are still evident. The relative error between the maximum observed wind gusts at each station and the corresponding maximum simulated gusts within a 36-hour window varies depending on the region.

In the Mauricie region, including Lac Memphrémagog, Granby, Lennoxville, and Trois-Rivières, CRCM6-1S performs poorly, underestimating gusts by 16.70% to 43.76% and overestimating them by 48.08% at Granby. Low average wind speeds (Figure 3a and 3b) in the region contribute to these underestimations. CRCM6-1L and CRCM6-2.5 also show poor performance, with similar or larger errors. CRCM6-12 demonstrates the best overall performance, with only Lennoxville as an outlier, while ERA5 reanalysis provides adequate results but generally underestimates gusts compared to the high-resolution simulations. These results highlight the importance of model resolution for accurately capturing both the magnitude and spatial variability of extreme wind gusts, particularly in regions with low average winds or unusual gust events.

For the Estuary stations (Cap-Chat, Mont-Joli, Baie-Comeau, and Pointe-au-Père), the simulations show improved performance compared to other regions. These stations, located near water, experience higher hourly winds due to their proximity to the St. Lawrence River. The relative error for CRCM6-1S ranges from −15.93% to 5.02% when compared to observations, indicating good performance with reasonable deviations. Similarly, CRCM6-1L and CRCM6-2.5 perform comparably, with very low errors. CRCM6-12 performs adequately, with errors ranging from −20.47% to 5.99%. Cap-Chat is slightly underestimated only by CRCM6-12 and ERA5, whereas CRCM6-1S and CRCM6-2.5 slightly overestimate the observed value.

The Outaouais stations (Ottawa, Montréal Mirabel, Maniwaki, and Saint-Jovite) do not show a clear overall behavior among CRCM6 simulations, with a wide range of relative errors from −50.17% to 22.14% for CRCM6-1S. The Ottawa station exhibits significant underestimation across all models due to the high wind gusts observed compared to the continuous wind. CRCM6-1L shows the best performance in the region, with the lowest relative errors. CRCM6-1S and CRCM6-2.5 perform adequately, while CRCM6-12 and ERA5 perform the worst, generally underestimating the gusts.

The Côte-Nord stations (Sept-Îles, Îles-aux-Perroquets, Havre-Saint-Pierre, and Natashquan) also do not display a clear trend, with over- and underestimations depending on the station and model. Overall, performance is below that of the other regions, with Îles-aux-Perroquets showing the largest underestimations. CRCM6-12 performs the worst, with errors ranging from −7.50% to −75.34%.

The absolute mean of the relative error shows that CRCM6-1S performs best, with 16.87%, although this statistic excludes the Côte-Nord region since it is outside the model domain. This exclusion likely contributes to the higher performance of this simulation. The ERA5 reanalysis follows with a mean relative error of 21.5%. Compared to the CRCM6 simulations, ERA5 is more conservative in its output, producing gusts within a narrower range across all stations. This results in consistent underestimation but also relatively higher performance in terms of mean relative error. CRCM6-2.5 shows a higher absolute mean error of 24.89%, indicating poorer performance when continuous hourly wind speeds are low. CRCM6-1L does not show improvement over CRCM6-2.5, with a mean relative error of 26.45%. CRCM6-12 performs the worst in this comparison, with an average relative error of 28.36%, largely influenced by two stations in the Côte-Nord region.

2.4 Discussion and conclusion

The goal of this study was to evaluate the capacity of the CRCM6 model to reproduce intense winds and gusts during destructive weather events. Specifically, we assessed the added value of high-resolution, convection-permitting simulations for mesoscale versus synoptic-scale storms. Hourly wind data from CRCM6 at multiple resolutions were compared with station observations to evaluate model performance. Metrics such as correlation, RMSE, bias, skill score, and relative difference were used to quantify the quality of both continuous wind and gust simulations and shown in Annex B. In this study, CRCM6 performance was assessed for two cases: a synoptic winter storm and a mesoscale derecho.

Overall, hourly winds were captured by CRCM6 across all resolutions. Consistent with previous studies, the skill of the WGE method was closely linked to the accuracy of simulated continuous winds (Brasseur, 2001; Stucki et al., 2016). Model performance was found to vary with horizontal resolution, station location, and the storm type analyzed. The synoptic storm was broadly well represented, though reduced performance was observed at stations located farther from large bodies of water and in regions experiencing weaker winds. More realistic wind speeds were also more consistently achieved with higher resolution. For the mesoscale storm, the simulations did not reproduce the intensity and variability observed over all regions. The higher resolution produced more realistic results with this mesoscale and rapidly evolving event.

When comparing the different horizontal resolutions, CRCM6-1S provides the most accurate wind estimates for both events, particularly in cases where complex atmospheric variability must be resolved, suggesting the added value of high-resolution result in more realistic wind speeds.

For the mesoscale storm in this study, no other model resolution was able to capture the wind field with comparable accuracy, and simulations at coarser resolutions show only moderate skill. Due to the nature of a derecho, the likelihood of accurately representing the event decreases as model resolution is reduced, leading to underestimated wind speeds and missed rapid wind peaks. Mesoscale storms remain challenging to simulate with the CRCM6 model. Correlations between stations and model resolutions were generally consistent, with station location exerting a similar influence as resolution.

In contrast, the synoptic-scale storm is characterized by a more gradual increase in continuous winds, allowing CRCM6 to represent the event more accurately across all resolutions. Under these conditions, the performance of CRCM6-1S is comparable to that of CRCM6-1L and CRCM6-2.5, as the larger spatial scale of the system reduces sensitivity to horizontal resolution. As a result, wind peaks and storm phases are captured by most model configurations, leading to improved overall wind estimates.

The gust analysis reveals substantial differences between the two case studies. The mesoscale derecho exhibits lower accuracy and predominantly negative relative errors, indicating a systematic underestimation of maximum wind gusts in this case. This event is less accurately represented by the model, and local-scale variability is insufficiently resolved. CRCM6-1S shows improved skill as with continuous winds in estimating maximum gusts compared to coarser model resolutions, as the finer grid spacing allows a better representation of the derecho and its associated small-scale, transient features and fast strengthening and weakening phases. In contrast, coarser resolutions have a limited ability to capture localized variations in wind patterns (Ágústsson & Ólafsson, 2009). With the synoptic event, the wind gust estimates were more realistic, and the variability was better represented. The model also had more difficulty when wind was low resulting in overestimation over the considered regions or stations.

The study nevertheless demonstrates strong potential for characterizing wind patterns at high-resolution in the CRCM6 model, particularly through its ability to reproduce the overall evolution and phases of wind speeds during the storm events. The limitations observed in the representation of the derecho event may also be partly related to uncertainties associated with station measurements. Given the rapid evolution and highly localized nature of peak wind gusts during the derecho event, observed winds can vary substantially over short spatial and temporal scales, potentially resulting in station records that underestimate the maximum winds that occurred locally.

In this study, CRCM6 performance was assessed for two cases: a synoptic winter storm and a mesoscale derecho. The model performs best in regions of stronger winds and at higher resolutions. The synoptic storm is more accurately represented due to its larger scale and smoother wind fields. However, factors such as spatial spin-up and wind direction were not analysed here, and their consideration could help explain the lower performance observed during the May 2022 storm and regional differences in model skill. More studies are needed to assess the capacity of the model to recreate winds in mesoscale events. The analysis of more case studies is needed to confirm the capacity of CRCM6 to simulate wind events. The use of spectral piloting in convection permitting could also be analyzed to determine its added value. More research on mesoscale events and changes in the configuration of the CRCM6 model would be useful in future works.

CHAPITRE 3 Discussion générale et conclusion

L'objectif principal de ce projet de maitrise était d'évaluer la capacité du modèle MRCC6 à reproduire les vents intenses et les rafales de vent associées à des événements météorologiques dommageables. Plus spécifiquement, cette étude visait à analyser la valeur ajoutée des simulations à très haute résolution spatiale (2,5 et 1 km) en mode *convection-permitting,* par rapport à des simulations réalisées à plus faible résolution (12 km). Dans ce contexte, différentes configurations du MRCC6 utilisant ces différentes résolutions ont été comparées à partir de simulations effectuées pour deux tempêtes, une de mésoéchelle et une autre d'échelle synoptique, qui ont affecté le sud du Québec en mai et décembre 2022 respectivement. Ces simulations ont été comparées et évaluées en utilisant les stations d'observation et la réanalyse ERA5.

Les résultats indiquent que le modèle MRCC6 est globalement capable de simuler de manière satisfaisante les vents horaires des tempêtes analysées. Ils montrent aussi que les vents intenses sont reproduits avec une précision acceptable par le modèle, bien que des différences subsistent selon le type d'événement.

La tempête synoptique est généralement mieux représentée que la tempête de mésoéchelle (Alpizar et al., 2026), laquelle n'est correctement simulée qu'aux résolutions les plus fines. Les simulations à très hautes résolutions utilisées dans cette étude se distinguent par des estimations plus précises des vitesses de vent et des rafales, par rapport aux valeurs observées. Pour les deux cas à l'étude, la résolution spatiale est importante pour la représentation des phénomènes atmosphériques intenses et potentiellement affectés par des facteurs locaux, notamment à proximité des reliefs et le long des zones de transition terre-mer, comme l'ont montré les résultats pour la région du Saguenay et l'Estuaire où le MRCC6 à plus haute résolution (2,5 et 1 km) présentait de meilleures performances que la simulation à plus basse résolution (12 km) ou la réanalyse ERA5. De manière générale, les régions situées à proximité des plans d'eau importants, comme le fleuve Saint-Laurent ou les Grands Lacs, présentent généralement une qualité de simulation supérieure pour les deux cas d'études. Par ailleurs, la présence de vents soutenus plus intenses favorise une meilleure représentation des rafales par le modèle (Brasseur, 2001), comme ce fut le cas le plus souvent pour les deux tempêtes analysées.

Par ailleurs, la taille du domaine, pour les simulations à 1 km, ne semble pas avoir un effet majeur sur les résultats, que ce soit pour les vents horaires ou les rafales de vent, et que ce soit pour le cas du derecho et de la tempête synoptique. Toutefois, une analyse détaillée de l'effet du *spin-up* spatial sur la qualité des simulations devrait être poursuivie, sachant que cela influence le développement de la convection (Matte et al., 2017) et la distribution des événements de précipitation selon l'éloignement de la limite du domaine (cf. Roberge et al., 2024).

L'analyse des simulations pour ces deux cas d'étude démontre une bonne capacité à reproduire les événements de manière générale. À plus faible résolution (i.e. avec le CRCM6-12), la variabilité et l'intensité des vents ne sont pas adéquatement capturées, toutefois, dans le cas de la tempête synoptique en particulier, les différentes phases de l'événement et leurs vents associés sont reproduites. Les périodes d'intensification et de dissipation de la tempête sont également bien représentées. Avec le raffinement de la résolution, soit pour les simulations CRCM6-2.5 et CRCM6-1L, la variabilité ainsi que l'intensité des vents sont mieux reproduites avec davantage de réalisme, de même que l'évolution spatiale à plus petite échelle. Finalement, pour la plus haute résolution et le petit domaine (celle du CRCM6-1S), l'intensité des vents ainsi que la variabilité spatiale et temporelle sont représentées de façon plus réaliste. Ces résultats sont cohérents avec les études récentes quant à la valeur ajoutée de la haute résolution, que ce soit pour la simulation des précipitations extrêmes (ex. Alpizar et al., 2026; Ghosh et al., 2025) ou dans le cas de systèmes météorologiques à l'origine de vents intenses (ex. Ma et al., 2025; Goyette et al., 2003).

L'analyse des directions des vents et des rafales mériterait également d'être approfondie pour confirmer la performance du modèle MRCC6. L'annexe C présente l'exemple d'une comparaison entre les directions des vents continus observés aux stations et celles simulées par le modèle à différentes résolutions. Les résultats montrent que, pour les deux cas étudiés, les simulations MRCC6-1S et MRCC6-2.5 reproduisent de manière satisfaisante les directions du vent (voir annexe C), tandis que la réanalyse ERA5 génère des directions moins précises ou plus éloignées des observations. Ce type d'analyse permettrait de valider plus rigoureusement la capacité du modèle à reproduire fidèlement les vents, non seulement en termes d'intensité, mais aussi de direction.

Cette étude demeure toutefois limitée par le nombre restreint de cas analysés, et la courte durée des simulations. L'inclusion d'autres cas de tempêtes de mésoéchelle pourraient en effet permettre de confirmer ou d'infirmer les résultats obtenus dans la présente étude. Des travaux futurs basés sur un ensemble plus large d'événements permettraient également de mieux évaluer les performances du MRCC6, en particulier selon la saison ou la période de l'année, et en mode climat historique et futur. Ceci permettrait d'améliorer notre compréhension et notre connaissance de la variabilité régionale et intra-saisonnière des vents intenses et des rafales et de leur changement dans le contexte des changements climatiques.

ANNEXE A

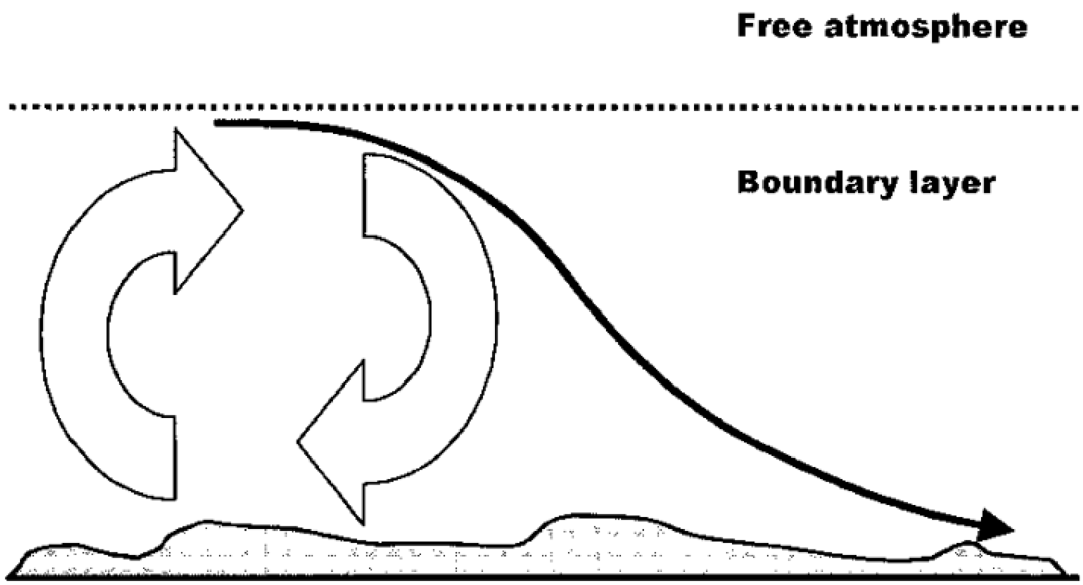

Figure A 1. Diagramme provenant de l'article Brasseur (2001) qui présente le mécanisme qui explique les rafales de vent observées à la surface.

ANNEXE B

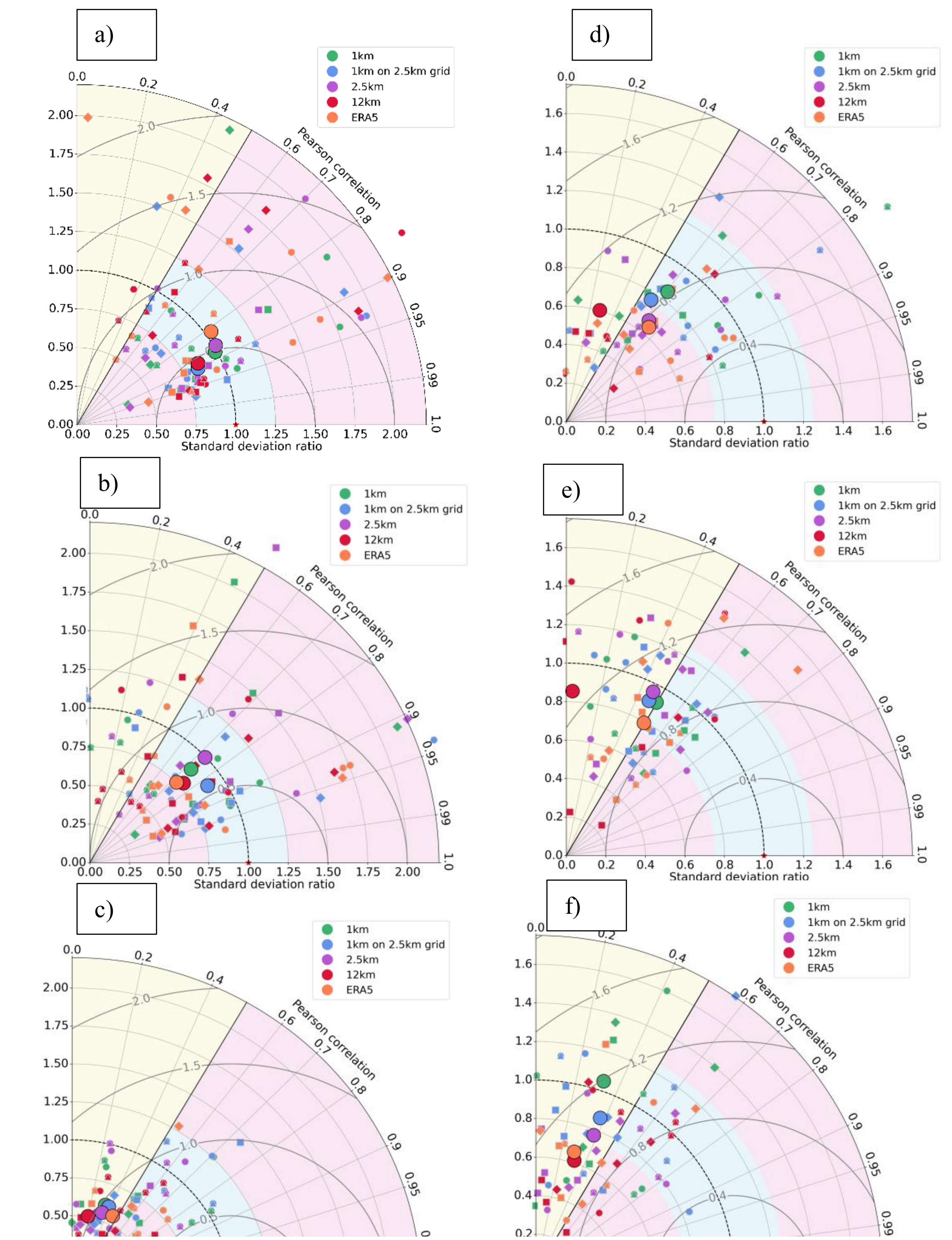

Figure B 1. a) Taylor diagram with Pearson correlation, standard deviation ratio and centered RMSE (solid circle line) for the simulations and reanalysis (Like Figure 4a). Added to the figure are small dot represents a data point of the 16 stations chosen at every hour and the bigger ones represent the average for every simulation (Excluding) Cote-Nord in the CRCM6-1S) in (a) 23 December (b) 24 December (c) 25 December (d) 20 May (e) 21 May (f) 22 May

ANNEXE C

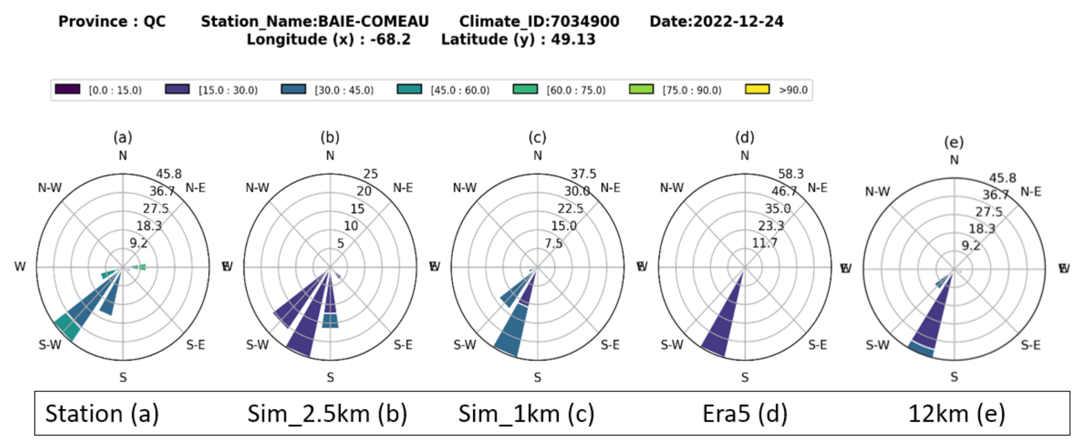

Figure C 1. Exemple d'une analyse de la direction des vents pour la station de Baie-Comeau le 24 décembre 2022. La force des vents horaires continus est codée selon un gradient de couleur allant du mauve (vents faibles) au jaune (vents forts) et la direction dans le cadran. Comparaison entre : (a) observations de la station, (b) simulation CRCM6-2.5 km, (c) simulation CRCM6-1S, (d) réanalyse ERA5 et (e) simulation CRCM6-12

BIBLIOGRAPHIE

Ágústsson, H. et Ólafsson, H. (2009). Forecasting wind gusts in complex terrain. *Meteorology and Atmospheric Physics*, *103*(1), 173-185. https://doi.org/10.1007/s00703-008-0347-y

Alpizar, M., Di Luca, A., Gachon, P. et al. (2026) Mesoscale Convective Systems in Northeastern North America: identification and evaluation with the convection-permitting version of the Canadian Regional Climate Model. *Clim Dyn* 64, 129. https://doi.org/10.1007/s00382-026-08102-6

Ashton, Arn. (2023). Anatomy of a Canadian Derecho: The Historic Derecho of May 21, 2022 [Présentation]. *Great Lakes Operational Meteorology Workshop*. https://www.ssec.wisc.edu/meetings/wp-content/uploads/sites/33/2023/06/Ashton_GLOMW-Derecho_Publish.pdf

Azorin-Molina, C., et al., (2017). Land surface wind speed [in "State of the Climate in 2016"]. *Bulletin of the American Meteorological Society*, *98*, S37-S39.

Azorin-Molina, C., et al., (2022). Land and ocean surface wind speed [in "State of the Climate in 2021"]. *Bulletin of the American Meteorological Society*, *103*(8), S71-S73.

Belušić, D. et Klaić, Z. B. (2004). Estimation of bora wind gusts using a limited area model. *Tellus A : Dynamic Meteorology and Oceanography*, *56*(4), 296-307. https://doi.org/10.3402/tellusa.v56i4.14425

Boettcher, F., Renner, C. H., Waldl, H. P. et Peinke, J. (2003). On the Statistics of Wind Gusts. *Boundary-Layer Meteorology*, *108*(1), 163-173. https://doi.org/10.1023/A:1023009722736

Born, K., Ludwig, P. et Pinto, J. G. (2012). Wind gust estimation for Mid-European winter storms: towards a probabilistic view. *Tellus A : Dynamic Meteorology and Oceanography*, *64*(1), 17471. https://doi.org/10.3402/tellusa.v64i0.17471

Bradbury, W. M. S., Deaves, D. M., Hunt, J. C. R., Kershaw, R., Nakamura, K., Hardman, M. E. et Bearman, P. W. (1994). The importance of convective gusts. *Meteorological Applications*, *1*(4), 365-378. https://doi.org/https://doi.org/10.1002/met.5060010407

Brasseur, O. (2001). Development and Application of a Physical Approach to Estimating Wind Gusts. *monthly Weather Review*, *129*(1), 5-25. https://doi.org/https://doi.org/10.1175/1520-0493(2001)129<0005:DAAOAP>2.0.CO;2

Catto, J. L., & Dowdy, A. (2021). Understanding compound hazards from a weather system perspective. *Weather and Climate Extremes*, *32*, 100313. https://doi.org/https://doi.org/10.1016/j.wace.2021.100313

Chai, R., Haynes, R. and Taber, B. (2023). A Review of the December 23-25, 2022 Multi Hazard Storm (High Winds, Flash Freeze/Snow Burst, and Heavy Lake Effect Snow with Blizzard Conditions). *NOAA, NWS*, https://www.weather.gov/btv/December-23-25th-Multi-Hazard-Storm#references

Changnon, S. A. (2009). Temporal and spatial distributions of wind storm damages in the United States. *Climatic Change*, *94*(3), 473-482. https://doi.org/10.1007/s10584-008-9518-6

Changnon, S. A. (2011). Windstorms in the United States. *Natural Hazards*, *59*(2), 1175-1187. https://doi.org/10.1007/s11069-011-9828-2

Cheng, C. S., et al., (2012). Possible Impacts of Climate Change on Wind Gusts under Downscaled Future Climate Conditions over Ontario, Canada. *Journal of Climate.*, *25*(1), 3390-3408.

Cheng, C. S., et al., (2014). Possible Impacts of Climate Change on Wind Gusts under Downscaled Future Climate Conditions: Updated for Canada. *Journal of Climate.*, *27*(3), 1225-1270.

Chilson, P. (2009). A First Course in Atmospheric Thermodynamics. *Eos, Transactions American Geophysical Union*, *90*. https://doi.org/10.1029/2009EO330005

Cholette, M., Laprise, R., & Thériault, J. M. (2015). Perspectives for Very High-Resolution Climate Simulations with Nested Models: Illustration of Potential in Simulating St. Lawrence River Valley Channelling Winds with the Fifth-Generation Canadian Regional Climate Model. *Climate*, *3*(2), 283-307. *of Geophysical Research: Atmospheres*, *108*(D13). https://doi.org/https://doi.org/10.1029/2002JD002646

Corfidi, S. F., (2003) Cold pools and MCS propagation: Forecasting the motion of downwind-developing MCSs. Wea. Forecasting, 18, 997–1017, https://doi.org/10.1175/1520-0434(2003)0182.0.CO;2.

Drazin, P. G. (2002). Introduction to Hydrodynamic Stability. Cambridge, UK: *Cambridge University Press*. https://ui.adsabs.harvard.edu/abs/2002ihs..book.....D

Environnement et Changement climatique Canada. (2023). *Technical Documentation Digital Archive of Canadian Climatological Data* (p. 37). Canada.

Fosser, G., Gaetani, M., Kendon, E. J., Adinolfi, M., Ban, N., Belušić, D., Caillaud, C., Careto, J. A. M., Coppola, E., Demory, M.-E., de Vries, H., Dobler, A., Feldmann, H., Goergen, K., Lenderink, G., Pichelli, E., Schär, C., Soares, P. M. M., Somot, S., & Tölle, M. H. (2024). Convection-permitting climate models offer more certain extreme rainfall projections. *Climate and Atmospheric Science*, *7*(1), 51. https://doi.org/10.1038/s41612-024-00600-w

Gachon, P. et Saucier, F. J. (2003). La modélisation du climat dans les mers intérieures du Canada : baie d'Hudson et golfe du Saint-Laurent. *Le Naturaliste canadien*, 127(2), 117–122. https://www.provancher.org/le-naturaliste-canadien/.

Gachon, P., Laprise, R., Zwack, P. et Saucier, F.J. (2003). The effects of interactions between surface forcings in the development of a model-simulated polar low in Hudson Bay. Tellus. Series A, Dynamic meteorology and oceanography, 55(1), 61–87. http://dx.doi.org/10.1034/j.1600-0870.2003.201267.x

Gatzen, C., Sills, D., Eng, S., Elliot, L., Jaffe, A., Miller, C., Gartner, M. et Kopp, G. (2025). Interpreting the damage from the 2022 Canadian derecho. *12th European Conference on Severe Storms*, Utrecht, The Netherlands. https://doi.org/https://doi.org/10.5194/ecss2025-316

Girard, C., Plante, A., Desgagné, M., McTaggart-Cowan, R., Côté, J., Charron, M., Gravel, S., Lee, V., Patoine, A., Qaddouri, A., Roch, M., Spacek, L., Tanguay, M., Vaillancourt, P. A. et Zadra, A. (2014). Staggered Vertical Discretization of the Canadian Environmental Multiscale (GEM) Model Using a Coordinate of the Log-Hydrostatic-Pressure Type. *Monthly Weather Review*, 142(3), 1183-1196. https://doi.org/https://doi.org/10.1175/MWR-D-13-00255.1

Ghosh, S., Lucas-Picher, P., Roy, P., Gachon, P. et Di Luca, A. (2025). Optimal Configuration of a Convection-Permitting Regional Climate Model in Simulating Precipitation Extremes: The Saguenay Flood. *Journal of Hydrometeorology*, *26*(11), 1751-1774. https://doi.org/https://doi.org/10.1175/JHM-D-25-0011.1

Gliksman, D., Averbeck, P., Becker, N., Gardiner, B., Goldberg, V., Grieger, J., Handorf, D., Haustein, K., Karwat, A., Knutzen, F., Lentink, H. S., Lorenz, R., Niermann, D., Pinto, J. G., Queck, R., Ziemann, A. et Franzke, C. L. E. (2023). Review article: A European perspective on wind and storm damage – from the meteorological background to index-based approaches to assess impacts. *Nat. Hazards Earth Syst. Sci.*, *23*(6), 2171-2201. https://doi.org/10.5194/nhess-23-2171-2023

Goyette, S., Brasseur, O. et Beniston, M. (2003). Application of a new wind gust parameterization: Multiscale case studies performed with the Canadian regional climate model. *J. Geophys. Res.*, *108*. https://doi.org/10.1029/2002JD002646

Gutowski, W. J., Ullrich, P. A., Hall, A., Leung, L. R., O'Brien, T. A., Patricola, C. M., Arritt, R. W., Bukovsky, M. S., Calvin, K. V., Feng, Z., Jones, A. D., Kooperman, G. J., Monier, E., Pritchard, M. S., Pryor, S. C., Qian, Y., Rhoades, A. M., Roberts, A. F., Sakaguchi, K., Zarzycki, C. (2020). The Ongoing Need for High-Resolution Regional Climate Models: Process Understanding and Stakeholder Information. *Bulletin of the American Meteorological Society*, *101*(5), E664-E683. https://doi.org/https://doi.org/10.1175/BAMS-D-19-0113.1

Hadavi, M., Sun, L. et Romanic, D. (2022). Normalized insured losses caused by windstorms in Quebec and Ontario, Canada, in the period 2008–2021. *International Journal of Disaster Risk Reduction*, *80*, 103222. https://doi.org/https://doi.org/10.1016/j.ijdrr.2022.103222

Hayashi, T. (1992). Gust and downward momentum transport in the atmospheric surface layer. *Boundary-Layer Meteorology*, *58*(1), 33-49. https://doi.org/10.1007/BF00120750

Henson, B. et Masters, J.(2022, 23 mai). At least 11 dead in wake of Michigan tornado, Canada derecho. *Yale Climate Connections*. https://yaleclimateconnections.org/2022/05/at-least-11-dead-in-wake-of-michigan-tornado-canada-derecho/

Hersbach, H., Bell, B., Berrisford, P., Hirahara, S., Horányi, A., Muñoz-Sabater, J., Nicolas, J., Peubey, C., Radu, R., Schepers, D., Simmons, A., Soci, C., Abdalla, S., Abellan, X., Balsamo, G., Bechtold, P., Biavati, G., Bidlot, J., Bonavita, M., Thépaut, J.-N. (2020). The ERA5 global reanalysis. *Quarterly Journal of the Royal Meteorological Society*, *146*(730), 1999-2049. https://doi.org/https://doi.org/10.1002/qj.3803

Houze, R. A., (2018). 100 years of research on mesoscale convective systems.A Century of Progress in Atmospheric and Related Sciences: Celebrating the American Meteorological Society Centennial, Meteor. Monogr., No. 59, *Amer. Meteor. Soc.*, https://doi.org/10.1175/AMSMONOGRAPHS-D-18-0001.1.

Hundecha, Y., St-Hilaire, A., Ouarda, T. B. M. J., El Adlouni, S., & Gachon, P. (2008). A Nonstationary Extreme Value Analysis for the Assessment of Changes in Extreme Annual Wind Speed over the Gulf of St. Lawrence, Canada. *Journal of Applied Meteorology and Climatology*, *47*(11), 2745-2759. https://doi.org/https://doi.org/10.1175/2008JAMC1665.1

HydroQuébec. (2022). *A look at the outages caused by the May 21 derecho* https://news.hydroquebec.com/en/press-releases/1841/a-look-at-the-outages-caused-by-the-may-21-derecho/

HydroQuébec (2). (2022). *Winter Storm - Hydro-Québec Provides an Update on the Outages*. https://news.hydroquebec.com/news/press-releases/all-quebec/hydro-quebec-provides-an-update-on-the-outages-1908.html

IPCC. (2023). Climate Change 2023 : Synthesis Report. Contribution of Working Groups I, II and III to the Sixth Assessment Report of the Intergovernmental Panel on Climate Change [Core Writing Team, H. Lee and J. Romero (eds.)]. IPCC, Geneva, Switzerland, pp. 35-115, doi: 10.59327/IPCC/AR6-9789291691647.

Jeong, D. I. et Sushama, L. (2019). Projected Changes to Mean and Extreme Surface Wind Speeds for North America Based on Regional Climate Model Simulations. *Atmosphere*, *10*(9). https://doi.org/10.3390/atmos10090497

Knox, J., Frye, J., Durkee, J. et Fuhrmann, C. (2011). Non-Convective High Winds Associated with Extratropical Cyclones. *Geography Compass*, *5*, 63-89. https://doi.org/10.1111/j.1749-8198.2010.00395.x

Kolendowicz, L., Taszarek, M. et Czernecki, B. (2016). Convective and non-convective wind gusts in Poland, 2001-2015. *Meteorology Hydrology and Water Management*, *4*, 15-21. https://doi.org/10.26491/mhwm/63636

Kurbatova, M., Rubinstein, K., Gubenko, I. et Kurbatov, G. (2018). Comparison of seven wind gust parameterizations over the European part of Russia. *Adv. Sci. Res.*, *15*, 251-255. https://doi.org/10.5194/asr-15-251-2018

Letson, F., Pryor, S. C., Barthelmie, R. J. et Hu, W. (2018). Observed gust wind speeds in the coterminous United States, and their relationship to local and regional drivers. *Journal of Wind Engineering and Industrial Aerodynamics*, *173*, 199-209. https://doi.org/https://doi.org/10.1016/j.jweia.2017.12.008

Llerena, A., Gachon, P. et Laprise, R. (2023). Precipitation Extremes and Their Links with Regional and Local Temperatures: A Case Study over the Ottawa River Basin, Canada. *Atmosphere,* 14(7), article 1130. http://dx.doi.org/10.3390/atmos14071130

Lu, Z., Han, Y., Liu, Y., Liu, S., Tang, Y., Liu, Z. et Wei, J. (2022). An improvement of wind gust estimate (WGE) method for squall lines. *Geomatics, Natural Hazards and Risk*, *13*(1), 993-1013. https://doi.org/10.1080/19475705.2022.2064773

Lucas-Picher, P., Argüeso, D., Brisson, E., Tramblay, Y., Berg, P., Lemonsu, A., Kotlarski, S., & Caillaud, C. (2021). Convection-permitting modeling with regional climate models: Latest developments and next steps. *WIREs Climate Change*, *12*(6), e731. https://doi.org/https://doi.org/10.1002/wcc.731

Ma, X., Li, Y. et Li, Z. (2022). The projection of canadian wind energy potential in future scenarios using a convection-permitting regional climate model. *Energy Reports*, *8*, 7176-7187. https://doi.org/https://doi.org/10.1016/j.egyr.2022.05.122

Ma, X., Li, Y., Huo, F. et Li, Z. (2025). Convection-permitting WRF simulation of extreme winds in Canada: Present and future scenarios. *Weather and Climate Extremes*, 49, 100777. https://doi.org/https://doi.org/10.1016/j.wace.2025.100777

Matte, D., Laprise, R., Thériault, J. M., & Lucas-Picher, P. (2017). Spatial spin-up of fine scales in a regional climate model simulation driven by low-resolution boundary conditions. *Climate Dynamics*, 49(1), 563-574. https://doi.org/10.1007/s00382-016-3358-2

Mccallum, E. et Norris, W. J. (1990). The storms of January and February 1990. *Meteorological Magazine*, *119*, 201-210.

McTaggart-Cowan, R., Vaillancourt, P. A., Zadra, A., Chamberland, S., Charron, M., Corvec, S., Milbrandt, J. A., Paquin-Ricard, D., Patoine, A., Roch, M., Separovic, L. et Yang, J. (2019). Modernization of Atmospheric Physics Parameterization in Canadian NWP. *Journal of Advances in Modeling Earth Systems*, *11*, 3593-3635. https://doi.org/https://doi.org/10.1029/2019MS001781

Minola, L. (2020). *Changes in near-surface winds across Sweden over the past decades – Observations and simulations* [University of Gothenburg]. Gothenburg, Sweden.

Minola, L., Zhang, F., Azorin-Molina, C., Pirooz, A. A. S., Flay, R. G. J., Hersbach, H. et Chen, D. (2020). Near-surface mean and gust wind speeds in ERA5 across Sweden: towards an improved gust parametrization. *Climate Dynamics*, *55*(3), 887-907. https://doi.org/10.1007/s00382-020-05302-6

Mohr, S., Kunz, M., Richter, A. et Ruck, B. (2017). Statistical characteristics of convective wind gusts in Germany. *Nat. Hazards Earth Syst. Sci.*, *17*(6), 957-969. https://doi.org/10.5194/nhess-17-957-2017

Moreno-Ibáñez, M., Laprise, R. et Gachon, P. (2023). Assessment of simulations of a polar low with the Canadian Regional Climate Model. *PLOS ONE*, 18(10), e0292250. https://doi.org/10.1371/journal.pone.0292250

Morris, M., Kushner, P. J., Moore, G. W. K. et Mercan, O. (2024). Resolution Dependence of Extreme Wind Speed Projections in the Great Lakes Region. *Journal of Climate*, 37(11), 3153-3171. https://doi.org/https://doi.org/10.1175/JCLI-D-23-0547.1

Munoz, A. B., & Anyomi, K. A. (2025). Windstorms in Ontario: 1950–2020. *Natural Hazards*, 122(1), 8. https://doi.org/10.1007/s11069-025-07856-2

Nakamura, K., Kershaw, R. et Gait, N. (1996). Prediction of near-surface gusts generated by deep convection. *Meteorological Applications*, *3*(2), 157-167. https://doi.org/https://doi.org/10.1002/met.5060030206

Pinto, J., et al., (2009). Assessment of the Wind Gust Estimate Method in mesoscale modelling of storms events over West Germany. *Meteorologische Zeitschrift*, *18*(5), 495-506.

Pletzer, A. et Fillmore, D. (2015). Conservative interpolation of edge and face data on n dimensional structured grids using differential forms. *Journal of Computational Physics*, *302*, 21-40. https://doi.org/https://doi.org/10.1016/j.jcp.2015.08.029

Poan, E.D., Gachon, P., Laprise, R., Aider, R. et Dueymes, G. (2018). Investigating added value of regional climate modeling in North American winter storm tracks simulations. *Climate Dynamics*, 50(5-6), 1799–1818. http://dx.doi.org/10.1007/s00382-017-3723-9

Pryor, S. C. et Barthelmie, R. J. (2010). Climate change impacts on wind energy: A review. *Renewable and Sustainable Energy Reviews*, *14*(1), 430-437. https://doi.org/https://doi.org/10.1016/j.rser.2009.07.028

Pryor, S. C., Nikulin, G. et Jones, C. (2012). Influence of spatial resolution on regional climate model derived wind climates. *Journal of Geophysical Research: Atmospheres*, *117*(D3). https://doi.org/https://doi.org/10.1029/2011JD016822

Roberge, F., Di Luca, A., Laprise, R., Lucas-Picher, P., & Thériault, J. (2024). Spatial spin-up of precipitation in limited-area convection-permitting simulations over North America using the CRCM6/GEM5.0 model. *Geosci. Model Dev.*, *17*(4), 1497-1510. https://doi.org/10.5194/gmd-17-1497-2024

Roderick, M. L., Rotstayn, L. D., Farquhar, G. D. et Hobbins, M. T. (2007). On the attribution of changing pan evaporation. *Geophysical Research Letters*, *34*(17). https://doi.org/https://doi.org/10.1029/2007GL031166

Sahin, S. et Türkeş, M. (2013). Contemporary surface wind climatology of Turkey. *Theoretical and Applied Climatology*, *113*(1), 337-349. https://doi.org/10.1007/s00704-012-0789-5

Samuelsson, P., Jones, C. G., Will´En, U., Ullerstig, A., Gollvik, S., Hansson, U., Jansson, E., Kjellstro¨M, C., Nikulin, G. et Wyser, K. (2011). The Rossby Centre Regional Climate model RCA3: model description and performance. *Tellus A: Dynamic Meteorology and Oceanography*, *63*(1), 4-23. https://doi.org/10.1111/j.1600-0870.2010.00478.x

Schumacher, R. S., & Rasmussen, K. L. (2020). The formation, character and changing nature of mesoscale convective systems. *Nature Reviews Earth & Environment*, *1*(6), 300-314. https://doi.org/10.1038/s43017-020-0057-7

Separovic, L., de Elía, R., & Laprise, R. (2012). Impact of spectral nudging and domain size in studies of RCM response to parameter modification. *Climate Dynamics*, *38*(7), 1325-1343. https://doi.org/10.1007/s00382-011-1072-7

Sheridan, P. (2018). Current gust forecasting techniques, developments and challenges. *Adv. Sci. Res.*, *15*, 159-172. https://doi.org/10.5194/asr-15-159-2018

Soh Y., Y. Hae, A. Mehmood, R. H. Ashraf, I. Kim (2013) Performance Evaluation of Various Functions for Kernel Density Estimation. *Open Journal of Applied Sciences*, vol. 3, pp. 58–64.

Son, J.-H., Franzke, C. L. E. et Son, S.-W. (2024). Dynamics of Extreme Surface Winds Inside North Atlantic Midlatitude Cyclones. *Geophysical Research Letters*, *51*(14), e2024GL110330. https://doi.org/https://doi.org/10.1029/2024GL110330

Steinheuer, J. et Friederichs, P. (2020). Vertical profiles of wind gust statistics from a regional reanalysis using multivariate extreme value theory. *Nonlin. Processes Geophys.*, *27*(2), 239-252. https://doi.org/10.5194/npg-27-239-2020

Stucki, P., Dierer, S., Welker, C., Gómez-Navarro, J., Raible, C., Martius, O. et Brönnimann, S. (2016). Evaluation of downscaled wind speeds and parameterised gusts for recent and historical windstorms in Switzerland. *Tellus A : Dynamic Meteorology and Oceanography*, *68*. https://doi.org/10.3402/tellusa.v68.31820

Taylor, K.E. (2001) Summarizing multiple aspects of model performance in a single diagram. *J. Geophys. Res.*, 106, 7183-7192,

Turner, R., Safaei Pirooz, A. A., Flay, R. G. J., Moore, S. et Revell, M. (2019). Use of High-Resolution Numerical Models and Statistical Approaches to Understand New Zealand Historical Wind Speed and Gust Climatologies. *Journal of Applied Meteorology and Climatology*, *58*(6), 1195-1218. https://doi.org/https://doi.org/10.1175/JAMC-D-18-0347.1

Večenaj, Ž., Belušić, D. et Grisogono, B. (2010). Characteristics of the near-surface turbulence during a bora event. *Ann. Geophys.*, *28*(1), 155-163. https://doi.org/10.5194/angeo-28-155-2010

Von Storch, H. and Zwiers, F. W. (2003). Statistical Analysis in Climate Research. Cambridge University Press, Cambridge.

Wakimoto, R. (2001). Convectively Driven High Wind Events. Dans *Severe Convective Storms* (p. 255-298). https://doi.org/10.1007/978-1-935704-06-5_7.

Węglarczyk S., Kernel density estimation and its application (2018). ITM web of conferences, vol. 23, EDP Sciences

Wilks, D. S. (2006). Statistical Methods in Atmospheric Sciences. 2nd edn. Elsevier, Amsterdam.

Whittaker, T., Di Luca, A., Roberge, F., & Winger, K. (2025). Evaluating Near-Surface Wind Speeds Simulated by the CRCM6-GEM5 Model Using AmeriFlux Data Over North America. *Journal of Advances in Modeling Earth Systems*, *17*(3), e2024MS004666. https://doi.org/https://doi.org/10.1029/2024MS004666

WMO, 2010, Measurements of surface wind, [in:] Guide to meteorological instruments and methods of observation, World Meteorological Organization, WMO-No. 8, Geneva, I.5 1-11

Xiang-E, L. et Xue-Liang, G. (2012). Role of Downward Momentum Transport in the Formation of Severe Surface Winds. *Atmospheric and Oceanic Science Letters*, *5*(5), 379-383. https://doi.org/10.1080/16742834.2012.11447020

Young, J. A. (2014). Static Stability. Dans F. Zhang (dir.), *Encyclopedia of Atmospheric Sciences* (vol. 2, p. 2114-2120). Elsevier Science. https://www.sciencedirect.com/referencework/9780123822253/encyclopedia-of-atmospheric-sciences

Zeng, Z., Ziegler, A. D., Searchinger, T., Yang, L., Chen, A., Ju, K., Piao, S., Li, L. Z. X., Ciais, P., Chen, D., Liu, J., Azorin-Molina, C., Chappell, A., Medvigy, D. et Wood, E. F. (2019). A reversal in global terrestrial stilling and its implications for wind energy production. *Nature Climate Change*, *9*(12), 979-985. https://doi.org/10.1038/s41558-019-0622-6